Acoustic wave equations and four ways media may perturb the speed of sound

version 1.3

Sverre Holm
Department of Physics
University of Oslo

16 January 2024

Contents

Chapter 1

Introduction

These notes have been written for the initial lectures in the Array Signal Processing course, IN5450, at the University of Oslo.

We start in Chap. 2 by deriving the lossless acoustic wave equation by distinguishing between conservation laws and constitutive laws. In the lossless case there is a constant speed of sound, $c = c_0$. What follows is structured around these four deviations from the lossless condition (first introduced in [Holm, 2019b, Sect. 2.3]):

1. $c = c' + \mathrm{i}c''$. **Attenuation** is implied when c is complex. Chap. 3, *Lossy wave equations*, shows that this is equivalent to a complex wave number. The chapter introduces classical lossy wave equations based on the viscous and the relaxation models.

   Chap. 4 *Power-law attenuation and complex media* gives an introduction to the important special case where the attenuation follows a power-law function of frequency. In complex media, the exponent is usually not an integer, and this may be modeled with fractional (non-integer) derivatives.

2. $c = c(\omega)$. **Dispersion** is when c varies with frequency. This is also covered in Chaps. 3 and 4 as attenuation and dispersion usually follow each other.

3. $c = c(p)$. **Nonlinearity** is where the amplitude of the pressure, p, influences the speed of sound. In Chap. 5 the fundamentals of nonlinear acoustics are presented

4. $c = c(x, y, z)$. **Refraction** is when c varies in space and this is covered in Chap. 6

This is followed by:

- Chap. 7 which gives the relationship between diffraction, convolution, and the spatial Fourier transform
- Chap. 8 which gives the background for simulation of acoustic fields based on the spatial impulse response or Green's function as well as on the angular spectrum

Some common approximations as well as a dictionary of common terms in Norwegian are in the Appendix.

1.1 Revision history

- ver 1.3, 16.01.2024:
  - Added chemical relaxation equation of (3.32).
  - Added middle term in denominator of Eq. (4.17).
  - Mentioned the Viscous Grain Shearing model on page 26.
  - Added description of relation between the spatial aperture domain and the wavenumber domain in Sect. 7.2.2.
  - Two first footnotes on page 44 added.
  - Minor corrections of text in several places.
- ver 1.2, 23.01.2023:
  - Added Sects. 3.1.2, 3.1.3, and 3.1.4 on Hookean and Newtonian materials
  - New derivations of lossy wave equations based on (3.10) in Sects. 3.3 and 3.4.1
  - Added discussion of soft glassy materials in Sect. 4.1
  - Linear time-invariant system assumption is specified in Sect. 5.3
  - Redone Fig. 5.4 for better clarity
  - Added (8.2) in the derivation of the Helmholtz equation
  - Corrected (8.15), added Fig. 8.1
  - Imaginary unit j changed to i and several other minor changes and additions
- ver 1.1, 22.01.2022:
  - Put power-law attenuation in separate Chap. 4 and expanded Sect. 4.1 with Fig. 4.2 and expanded Sect. 4.2 on fractional models
  - Minor changes:
    * Homogeneous medium assumption in footnote on page 4
    * Possible upper limit for speed of sound at the end of Sect. 2.2.1
    * Discussed complex frequency at the end of Sect. 3.2.1
    * Geometrical acoustics assumption on page 33
- ver 1.0, 14.01.2022: Initial version

1.2 Typesetting

This document has been typeset using LaTeX and the *BYUTextbook.cls* class file (modified for A4 paper size) used in the online textbook [Peatross and Ware, 2015] from the Optics Education Group, Department of Physics and Astronomy, Brigham Young University.

Chapter 2

The lossless wave equation

This chapter covers the derivation of the lossless wave equation and its solution in the form of plane waves. The equation is also given in spherical coordinates. The Helmholtz equation, which is a space-only version of the wave equation is then found and the basis for simulation methods based on the spatial impulse response or Green's function as well as the angular spectrum are given.

Sections 2.1-2.2 have been extracted from [Holm, 2019b, Chap. 2.1 and B.1].

2.1 The acoustic wave equation

This section and Sec. 3.1 cover much of the same material, but here the derivation is more rigorous than in Sec. 3.1. It may therefore be an advantage to read Section 3.1 before this section.

Let the pressure and the density be composed of a static value plus a perturbation:

$$p' = p_0 + p, \tag{2.1}$$

$$\rho' = \rho_0 + \rho. \tag{2.2}$$

The derivation of the lossless acoustic wave equation starts from Euler's equation. It expresses ***conservation of momentum***:

$$\rho' \frac{\mathrm{D}\vec{v}}{\mathrm{D}t} = \rho' \left(\frac{\partial \vec{v}}{\partial t} + \vec{v} \cdot \nabla \vec{v} \right) = -\nabla p', \tag{2.3}$$

where $\vec{v}$ is the fluid velocity which relates to displacement, $\vec{u}$ via $\vec{v} = \partial \vec{u} / \partial t$. The operator ∇ is the grad operator. Here the total, material, or substantial time derivative which is connected with the moving substance, is:

$$\frac{\mathrm{D}}{\mathrm{D}t} = \frac{\partial}{\partial t} + \vec{v} \cdot \nabla \tag{2.4}$$

The second conservation equation is the ***conservation of mass*** principle expressed in the equation of continuity. It states that the net influx of matter into a volume element is reflected in a change of density:

$$\frac{\partial \rho'}{\partial t} + \nabla \cdot (\rho' \vec{v}) = \frac{\partial \rho'}{\partial t} + \rho' \nabla \cdot \vec{v} + \vec{v} \cdot \nabla \rho' = \frac{\mathrm{D}\rho'}{\mathrm{D}t} + \rho' \nabla \cdot \vec{v} = 0, \tag{2.5}$$

where $\nabla \cdot$ is the div operator. Euler's equation and the equation of continuity are illustrated and explained in more detail in [Kinsler et al., 1999, Chap. 5].

The derivation of the acoustic wave equation builds on pressure, p, and density, ρ, variations around equilibrium or static values p_0 and ρ_0. The

variations are assumed to be small and with a fluid velocity which is much smaller than the speed of sound:

$$p \ll p_0, \quad \rho \ll \rho_0, \quad |\vec{v}| \ll c. \tag{2.6}$$

Therefore Euler's equation may be linearized by equating the material and partial derivatives. Likewise the continuity equation may be linearized by neglecting the gradient of the density.[1] The approximate equations are:

$$\textit{Linearized conservation of momentum:} \quad \rho_0 \frac{\partial \vec{v}}{\partial t} = -\nabla p, \tag{2.7a}$$

$$\textit{Linearized equation of continuity:} \quad \frac{\partial \rho}{\partial t} + \rho_0 \nabla \cdot \vec{v} = 0. \tag{2.7b}$$

The third equation is the ***constitutive equation*** or equation of state. It comes from a special case of the ideal gas equation, $p' V^\gamma = C$, where γ is the adiabatic gas constant or heat capacity ratio, and C is a constant. Since the density is inverse proportional to volume, V, the gas law can be rewritten as $(p_0 + p)/p_0 = (\rho_0 + \rho)/\rho_0)^\gamma$. Hooke's law is a linearization around the static pressure p_0:

$$p = K \frac{\rho}{\rho_0}, \quad K = \gamma p_0. \tag{2.8}$$

K is the bulk modulus, the inverse of the compressibility. This derivation builds on [Landau and Lifshitz, 1987, Chaps. I § 1-2 and VIII § 64] and [Hamilton and Blackstock, 2008, Chap. 3].

Substituting the divergence of (2.7a) in the time derivative of (2.7b) gives a second order equation involving p and ρ. Replacing ρ by p using (2.8) results in the lossless wave equation:

$$\nabla^2 p - \frac{1}{c_0^2} \frac{\partial^2 p}{\partial t^2} = 0, \tag{2.9}$$

where the speed of sound is:

$$c_0 = \sqrt{K/\rho_0}. \tag{2.10}$$

This derivation assumes that the medium is homogeneous so that the density, ρ, or the bulk modulus, K, do not vary in space.

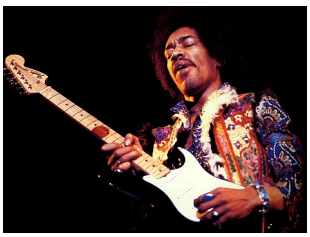

Jimi Hendrix (1942-1970) American musician who was one of the most influential electric guitarists in the history of popular music. He is described by The Rock and Roll Hall of Fame as "arguably the greatest instrumentalist in the history of rock music". The wave equation for the string, such as in the guitar, was the first one to be formulated (http://classicrock.wikia.com/).

2.2 Properties of the lossless wave equation

The lossless wave equation on vector form is:

$$\nabla^2 \vec{u} - \frac{1}{c_0^2} \frac{\partial^2 \vec{u}}{\partial t^2} = 0. \tag{2.11}$$

In acoustics $\vec{u}$ is the displacement vector. It may also be replaced by the scalar pressure p. In elastic wave propagation it can be the shear displacement, and in electromagnetics $\vec{u}$ should be replaced by the electric or the magnetic field.

[1] This term cannot be neglected in nonlinear acoustics, see Chap. 5 nor in inhomogeneous media, see [Holm, 2019b, Chap. 9.2].

Example 2.1 The lossless wave equation. Even the lossless equation fits remarkably well to reality, especially for the two most important modes for humans: acoustics of audible sound in air and propagation of the electromagnetic waves of visible light.

Radio communications in the VHF (30–300 MHz) and UHF (300–3000 MHz) ranges can also be considered to be lossless, at least under line-of-sight conditions. That covers such important applications as radio and TV broadcasting, as well as cellular phones.

In the 1-D case of a string, such as a guitar string, one can think of u as the displacement as shown in Fig. 2.1. If the string is pulled up, the second order spatial derivative will be negative, i.e. the first term in the wave equation. The second term of the lossless wave equation is proportional to the second order temporal derivative, i.e. the acceleration. The equation in this example says that acceleration is negative, i.e. downwards. So the result is that the string will shift from being pulled up to move towards the neutral position. As it moves beyond the equilibrium, its second order derivative shifts sign, and therefore also the acceleration. And so the movement keeps reinforcing itself.

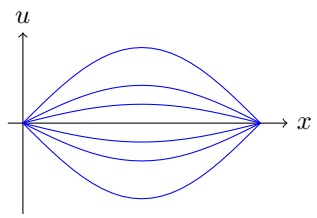

Figure 2.1 A string which is pulled up from the equilibrium position will oscillate

2.2.1 Monochromatic plane wave

We start by assuming that the wave equation has a solution in time at a single frequency (an eigenmode), i.e. $u_t(t) = \exp(\mathrm{i}\omega t)$. The rest of the solution then only depends on space and under free-field conditions it turns out that the spatial variables have independent solutions, i.e. the solution is separable $\vec{u}(x, y, z, t) = A \cdot u_t(t) \cdot u_x(x) \cdot u_y(y) \cdot u_z(z)$, where A is an arbitrary real constant. This also implies that the solution is a complex exponential in each of the spatial dimension, i.e. that it is a plane wave $u_x(x) = \exp(-\mathrm{i}k_x x)$. That gives the following solution:

$$\vec{u}(\vec{x}, t) = A\exp\{\mathrm{i}(\omega t - k_x \cdot x - k_y \cdot y - k_z \cdot z)\} = A\exp\{\mathrm{i}(\omega t - \vec{k} \cdot \vec{x})\}, \tag{2.12}$$

where $|\vec{k}|$ is the wavenumber. In general it is a vector, and for the lossless wave equation, each of its components, k_x, k_y, k_z are real.

When this solution is inserted in the wave equation of (2.11) the result is the dispersion relation which relates k and ω. In 1-D it is:

$$\begin{aligned}(-\mathrm{i}k)^2 u(x, t) &= \frac{1}{c_0^2}(\mathrm{i}\omega)^2 u(x, t) \\ k^2 = \frac{\omega^2}{c_0^2} \quad &\text{or} \quad k = \frac{\omega}{c_0} = \frac{2\pi f}{c_0} = \frac{2\pi}{\lambda},\end{aligned} \tag{2.13}$$

where f is the frequency and λ is the wavelength. In the lossless case there is a simple linear relation between the angular frequency, ω and the magnitude of the wave vector.

The dispersion equation is one of the most important tools for analyzing more complex forms of the wave equation.

The solution to the wave equation can alternatively be expressed as:

$$\begin{aligned} u(\vec{x}, t) &= A\exp\{\mathrm{i}(\omega t - \vec{k}\cdot\vec{x})\} \\ &= A\exp\{\mathrm{i}\omega(t - \vec{s}\cdot\vec{x})\} = u(t - \vec{s}\cdot\vec{x}). \end{aligned} \tag{2.14}$$

The vector $\vec{s} = \vec{k}/\omega$ has the property $|\vec{s}| = 1/c_0$. This is the slowness vector. It points in the direction of propagation and has units of reciprocal velocity (s/m). It is equivalent to the optical index of refraction, $n = c_{vac}/c_0$, except that there is no equivalent to the free-space propagation speed in vacuum, c_{vac}, in acoustics. There are however those that argue that there might even be an upper limit for the speed of sound which depends on fundamental material properties [Trachenko et al., 2020].

2.2.2 The wave equation in spherical coordinates

Under the assumption that the solution exhibits spherical symmetry, the wave equation in Cartesian coordinates, (2.11) can be transformed to:

$$\frac{1}{r^2}\frac{\partial}{\partial r}\left(r^2\frac{\partial u}{\partial r}\right) = \frac{1}{c_0^2}\frac{\partial^2 u}{\partial t^2}, \tag{2.15}$$

where r is the distance from the source. It has a spherical wave solution, which for the monochromatic case is:

$$u(r, t) = \frac{C}{r}\exp\{\mathrm{i}(\omega t - kr)\}. \tag{2.16}$$

where C is an arbitrary real constant.

This solution propagates away from origin. Another solution propagating towards the origin is found by replacing '-'with '+'. It may also be valid, and it is the boundary conditions which determine which ones exist.

The attenuation due to the factor $1/r$ is due to the spread of the energy over a larger and larger sphere around the source. It does not represent a loss of energy (absorption), only a loss of energy density.

Chapter 3

Lossy wave equations

3.1 Conservation laws and constitutive equations

When the lossy wave equation was derived in the previous chapter it was found by combining conservation principles derived from space-time symmetries with the material's constitutive equation as shown in Fig. 3.1. This will be elaborated in this chapter and a brief introduction to viscous and relaxation models for loss will be given.

This chapter builds on Chaps. 1.2 and 2.3-2.6 of [Holm, 2019b]

3.1.1 Conservation principles

In acoustics and elastic wave propagation, the equation that expresses conservation of linear momentum is an expression for Newton's second law which relates force, mass and acceleration: $F = ma$. It can also be stated as $F = \mathrm{d}(mv)/\mathrm{d}t$ where the linear momentum, mv, is the product of mass and velocity. Linearized conservation of linear momentum in a closed system, which is related to the Euler equation in fluid dynamics, is usually stated as the equivalence between the rate of change of momentum per volume and the negative gradient of the pressure or the average force over a unit volume:

$$\rho_0 \frac{\partial \mathbf{v}}{\partial t} = -\nabla p. \tag{3.1}$$

where ρ_0 is equilibrium density, $\mathbf{v}$ is the velocity vector and p is the pressure. Conservation of linear momentum is a fundamental principle of physics which derives from the principle of symmetry in space first expressed by Noether (see sidebar).

The second principle is concerned with energy conservation in a closed system. At rest (non-relativistic) it is the same as conservation of mass via $E = mc^2$ [Feynman, 1967], and local conservation of mass is expressed in the continuity equation. After linearization, it states that the rate at which mass enters a closed system in steady state is equal to the volume expansion rate:

$$\frac{\partial \rho}{\partial t} + \rho_0 \nabla \cdot \mathbf{v} = 0. \tag{3.2}$$

The underlying principle of conservation of energy is Noether's theorem of symmetry in time. More exact versions of (3.1) and (3.2) are found in Sect. 2.1.

The conservation principles are valid in a closed system. This is assumed here. It implies that energy converted by absorption can be recovered or that the loss is so small compared to the total energy that the effect is minor. A different case is when absorption removes significant energy from the system in an irreversible way. Then it is an open system and the time-irreversible

Emmy Noether (1882–1935) German mathematician. During her studies in Erlangen from 1900 she was not allowed to participate fully in classes as a woman and when teaching in Göttingen from 1915 she was not allowed to hold an official position. However, the end of World War I brought changes for women's rights. She spent 1928-29 in Moscow and in addition to her Jewish background this contributed to her expulsion from her position in Göttingen and emigration to USA in 1933. In theoretical physics she is known for Noether's theorem which connects symmetries and conservation laws:

- Conservation of linear momentum is a consequence of invariance to spatial translation
- Conservation of energy is a consequence of invariance under time translations
- Conservation of angular momentum is due to invariance with respect to rotation

See [Landau and Lifshitz, 1976, Chap. II] for derivations. Noether built on the theory of Lie groups developed by the Norwegian mathematician Sophus Lie (1842-1889) who was a professor in Leipzig and Oslo. Image: Public domain, from Wikipedia Commons. (Wikipedia)

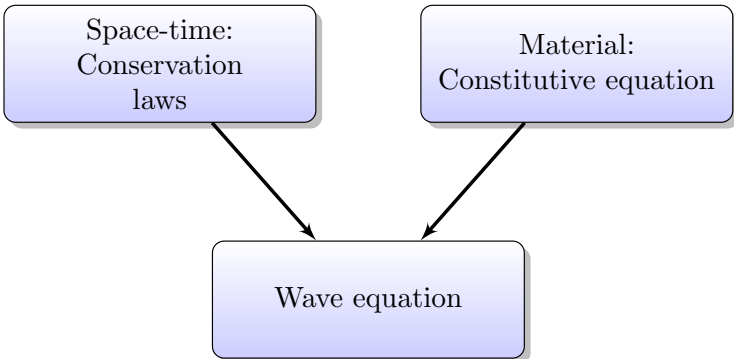

Figure 3.1 A wave equation is found by combining space-time conservation principles with the material's constitutive equation

mechanism is not conservative. This may lead to different conservation principles [Riewe, 1996].

Apart from such a case, the conservation principles relate to the properties that an experiment may be performed in a different place with the same result—symmetry in space—or performed at a different time with the same outcome—symmetry in time [Gross, 1996]. These are properties which are at the foundation of physics [Feynman, 1967] and many would say that what they describe is so obvious that one rarely needs to think about it. Such statements, which are accepted without controversy, are usually called axioms, and as such belong to what one may call meta-science. Axioms are mostly known from mathematics, and not in so many other sciences. Physics may be an exception, as space- and time-invariance can be considered to have an axiomatic standing. This was also the view in one of the earliest statements of the philosophy of science written by the mathematics professor Roger Cotes (1682-1716). He had urged Newton to issue a second edition of the Principia, which he later edited and wrote the preface for (1713):

> The foregoing conclusions are grounded on this *axiom*, which is received by all philosophers; namely that effects of the same kind; that is, whose known properties are the same, take their rise from the same causes and have the same unknown properties also. For who doubts, if gravity be the cause of the descent of a stone in Europe, but that it is also the cause of the same descent in America? If there is a mutual gravitation between a stone and the Earth in Europe, who will deny the same to be mutual in America? If in Europe, the attractive force of a stone and the Earth is compounded of the attractive forces of the parts; who will deny the like composition in America? If in Europe, the attraction of the Earth be propagated to all kinds of bodies and to all distances; why may it not as well be propagated in like manner in America? All philosophy is founded on this rule; for if that be taken away we can affirm nothing of universals. The constitution of particular things is known by observations and experiments; and when that is done, it is by this rule that we judge universally of the nature of such things in general. [italics added]

3.1.2 Hookean and Newtonian medium models

To understand attenuation of waves, it is necessary also to consider models of linear viscoelasticity where the central concept is the constitutive equation. The two elementary building blocks of the conventional constitutive equations are the spring and the damper. These models both have their roots in the 17th century.

Lossless propagation is based on a constitutive equation which states that for an ideal spring, force and compression are proportional. It was first stated in 1660 by Robert Hooke. For an ideal gas, this means that pressure, p, and density, ρ, are proportional:

$$p = K\frac{\rho}{\rho_0}, \quad K = \gamma p_0, \tag{3.3}$$

where K is the elastic modulus, γ is the adiabatic gas constant, and ρ_0 and p_0 are equilibrium density and pressure respectively. This is a linearization of the gas law of (5.1).

Pressure is force per area and here the terminology will follow that of linear viscoelasticity where in the lossless case, stress is negative pressure, $\sigma = -p$. Thus stress represents internal forces in the medium measured per area and with unit Pa/m^2. The second variable in the constitutive law is strain which represents the medium's extension from an equilibrium position. It is dimensionless and is the ratio of the extension and the original length. It can also be written as $\varepsilon = -\rho/\rho_0$. Then Hooke's law, assuming infinitesimal strains and stresses, expresses a linear relationship between them:

$$\sigma_S(t) = E\varepsilon(t), \tag{3.4}$$

where E is a generic elastic modulus and the subscript S means spring.

A Newtonian fluid also has a stress component which is proportional to the velocity gradient according to a brief statement by Newton in Principia in 1687:

$$\sigma_D(t) = \eta\frac{\partial v}{\partial x} = \eta\frac{\partial}{\partial t}\frac{\partial u}{\partial x}, \tag{3.5}$$

where η is a generic viscosity, $v = \partial u/\partial t$ is velocity, and u is displacement. Today this is expressed in tensor form, but Newton's original statement was more like the 1-D version above. Substituting $\varepsilon = \partial u/\partial x$, which is an expression of conservation of mass, (3.2) reformulates Newton's original statement into one between stress and strain:

$$\sigma_D(t) = \eta\frac{\partial \varepsilon(t)}{\partial t}. \tag{3.6}$$

This is the most common description of viscosity: a stress component which is proportional to velocity. It can be interpreted as a damper where the faster the movement, the more the movement meets resistance, hence the subscript D. This resistance is one of the main causes of attenuation for propagating waves.

3.1.3 Constitutive equations

A constitutive equation is different from a conservation law because of its empirical nature. Hooke's law and the law for Newtonian viscosity are primarily based on measurements of material characteristics, although they can be justified in some underlying physical principle as well. But these principles are not as fundamental as the symmetry principles behind the conservation laws. This is one of the lessons to be learned from a study of linear viscoelasticity.

The constitutive equation, or stress–strain relation, can be expressed by means of the dynamic modulus, $\tilde{E}(\omega)$, in the frequency domain. In the Hookean case of (3.4), it is $\tilde{E}(\omega) = E$, and in the Newtonian case of (3.6), it is $\tilde{E}(\omega) = \mathrm{i}\eta\omega$. The lossy models combine these elements in various ways.

3.1.4 Dispersion equation from dynamic modulus

In the rest of these lecture notes, the wave equation will be found directly from the dynamic modulus, $\tilde{E}(\omega)$. This is built on transforming the main equations to the frequency domain. The constitutive equation is then

$$\tilde{\sigma}(\omega) = \tilde{E}(\omega)\tilde{\varepsilon}(\omega). \tag{3.7}$$

The frequency domain version of the conservation of momentum is:

$$\rho_0 \frac{\partial^2 u}{\partial t^2} = \nabla\sigma \quad \Leftrightarrow \quad \rho_0 (\mathrm{i}\omega)^2 \tilde{u}(\omega) = -\mathrm{i}k\,\tilde{\sigma}(\omega), \tag{3.8}$$

and conservation of mass gives:

$$\varepsilon(t) = \frac{\partial u}{\partial x} \quad \Leftrightarrow \quad \tilde{\varepsilon}(\omega) = -\mathrm{i}k\,\tilde{u}(\omega). \tag{3.9}$$

Now insert (3.9) in (3.7) to eliminate $\tilde{\varepsilon}(\omega)$ and then use (3.8) to eliminate $\tilde{u}(\omega)$. The wave number is then:

☜ Will be used later!

$$k^2(\omega) = \frac{\rho_0\omega^2}{\tilde{E}(\omega)}. \tag{3.10}$$

All subsequent wave equations in this chapter will be found from this relation.

As an example, the lossless case has $\tilde{E}(\omega) = E$, and when inserted in (3.10) this gives the dispersion relation as:

$$k^2 = \frac{\rho_0\omega^2}{E} = \frac{\omega^2}{c_0^2}, \quad c_0^2 = \frac{E}{\rho_0}, \tag{3.11}$$

which is the one given in (2.13).

3.2 Characterization of attenuation

The specific form of attenuation which is absorption occurs when the energy in the wave is converted into some other form of energy, most often heat. It can both be in the form of viscous losses or in the form of relaxation losses. The latter is due to a conversion of kinetic or translational energy of the molecules into internal energy. In medical ultrasound scattering may contribute from 2-30 % or so of the total attenuation, at least at low frequencies

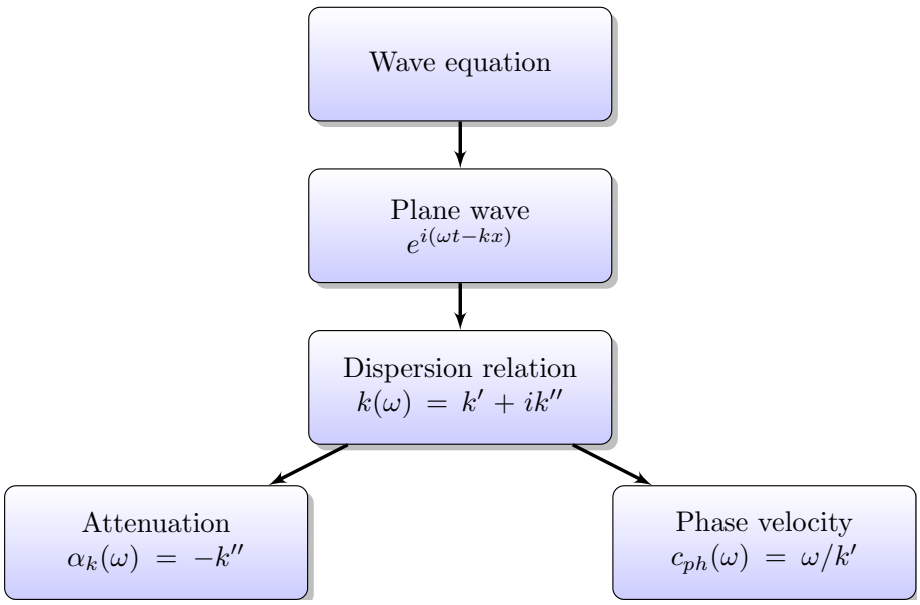

Figure 3.2 Finding the dispersion relation, and attenuation and phase velocity from a wave equation, (adapted from [Blackstock, 2000, Fig. 9.1])

(<10–15 MHz) [Bamber, 2004], so absorption is the dominant loss mechanism. Other media with much lower attenuation than in medical ultrasound, such as ultrasound in air or in underwater acoustics, are also described by absorption.

3.2.1 Dispersion relation

In order to analyze attenuation, the scheme depicted in Fig. 3.2 is followed. This method goes at least back to [Stokes, 1845]. A unit amplitude plane wave solution is assumed and inserted into the wave equation resulting in a dispersion equation. That procedure was in fact already used in order to arrive at the lossless dispersion relation of (2.13).

The main difference from the lossless case is that an attenuating wave is characterized by a complex wavenumber $k = k' + \mathrm{i}k''$. This can be seen by inserting a complex wavenumber into the 1-D solution of (2.12):

$$u(x,t) = A\exp\{\mathrm{i}(\omega t - k\cdot x)\} = A\exp\{k''\cdot x\}\cdot\exp\{\mathrm{i}(\omega t - k'\cdot x)\}. \tag{3.12}$$

The real part of k represents propagation as it is found in the complex exponential. It also defines the phase velocity, $k' = \omega/c_{ph}$. The imaginary part represents attenuation: $\alpha_k = -k''$. Together this gives:

$$k = k' + \mathrm{i}k'' = \frac{\omega}{c_{ph}(\omega)} - \mathrm{i}\alpha_k(\omega), \tag{3.13}$$

Very often the attenuation will follow a power law:

$$\alpha_k = -k'' = a_0|\omega|^y. \tag{3.14}$$

In practice propagating waves are not plane waves, except very far away from the source. A more realistic model near a source is a spherical wave and then spherical spreading loss from (2.16) and attenuation may be combined:

$$u(r,t) = \frac{C}{r}\exp\{-\alpha_k \cdot r\}\exp\{\mathrm{i}(\omega t - k' r)\} \tag{3.15}$$

Further the attenuation factor, α_k, may have several causes and one of the challenges in distinguishing between viscous absorption and losses due to scattering is that they may behave similarly with respect to power-law characteristics.

In the first part of this chapter, attenuation due to viscosity and relaxation are discussed. That corresponds to losses described primarily by $y = 2$ and secondarily by $y = 0$ and $y = 0.5$ in (3.14).

Deviations from a lossless medium

There may also be other deviations from a lossless medium than attenuation. Common deviations from a lossless, homogeneous medium are in addition dispersion, nonlinearity, and refraction. They manifest themselves in different ways and a coherent way to express them is by the way they affect the propagation speed:

1. Attenuation: $c = c' + \mathrm{i}c''$ is complex
2. Dispersion: $c = c(\omega)$ varies with frequency
3. Nonlinearity: $c = c(p)$ depends on amplitude of the pressure, p (Chap. 5)
4. Refraction: $c = c(x, y, z)$ varies in space (Chap. 6)

Attenuation and dispersion usually follow each other. Linear, homogeneous media will be assumed in this chapter.

The **imaginary propagation speed** may need an explanation. Let the propagation speed be imaginary, for instance due to an imaginary elastic modulus, and insert into the dispersion relation from (2.13):

$$k = \frac{\omega}{c} = \frac{\omega}{c' + \mathrm{i}c''} = \frac{\omega}{c'^2 + c''^2}(c' - \mathrm{i}c'') = \frac{\omega}{|c|^2}(c' - \mathrm{i}c'') = k' + \mathrm{i}k''. \tag{3.16}$$

Therefore the real and imaginary parts of c and k correspond to each other and a complex propagation speed, c, is the same as having a complex wavenumber.

Likewise, the combination of a **complex frequency** and a real wavenumber are sometimes used [Holm, 2019a] (but not in these lecture notes). To see the equivalence, consider $\omega = \omega' + \mathrm{i}\omega''$ in the propagating wave:

$$u(x,t) = A\exp\{\mathrm{i}(\omega t - k \cdot x)\} = A\exp\{\omega'' \cdot t\} \cdot \exp\{\mathrm{i}(\omega' t - k \cdot x)\}. \tag{3.17}$$

Thus the imaginary part of the frequency describes damping. Further comparison with $k = k' + \mathrm{i}k'' = \omega / c(\omega) - \mathrm{i}\alpha_k$ gives:

$$\alpha_k = -\frac{t}{x}\omega'' = -c(\omega)\omega''. \tag{3.18}$$

3.3 The viscous wave equation

The viscous wave equation is based on a constitutive model where elasticity and viscosity are added:

$$\tilde{E}(\omega) = E + \mathrm{i}\eta\omega. \tag{3.19}$$

Inserted in (3.10) gives this dispersion relation in 1-D:

$$k^2 - \frac{\omega^2}{c_0^2} + \mathrm{i}\omega\tau k^2 = 0, \quad \tau = \eta/E, \tag{3.20}$$

The result is that an attenuation term is added to the wave equation, giving:

$$\nabla^2 \vec{u} - \frac{1}{c_0^2}\frac{\partial^2 \vec{u}}{\partial t^2} + \tau\frac{\partial}{\partial t}\nabla^2 \vec{u} = 0. \tag{3.21}$$

This equation was first given by [Stokes, 1845, p. 302] and it describes absorption in for instance distilled water, see Sec. 3.5.1.

The wave equation of (3.21) can be derived in two different ways, either from the spring-damper model, as just done from (3.19) and shown in Fig. 3.3 and explained below, or from the Navier-Stokes equation.

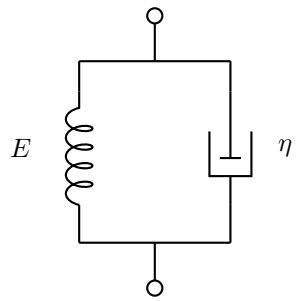

Figure 3.3 Kelvin-Voigt constitutive model

3.3.1 Derivation from a spring-damper model

We employ a simplified elastic model which assumes that only one mode, either a compressional or a shear mode, is present at any one time. The medium is also assumed to have the same properties everywhere (homogeneous) and be independent of direction (isotropic).

The parameters of the model are E which is the elastic modulus, η which is the viscosity, and $\tau = \eta/E$ which is a retardation time given by their ratio. Note that the E of the Kelvin-Voigt model is not the same as the Young's modulus, but a generic parameter which changes meaning depending on the wave mode. Also the η of the Kelvin-Voigt model is only the same as the shear modulus in case of shear waves, but not for the pressure elastic wave or in acoustics.

In the Kelvin-Voigt model, the stresses add:[1]

$$\sigma(t) = E\varepsilon(t) + \eta\frac{\partial\varepsilon(t)}{\partial t} = E\left[\varepsilon(t) + \tau\frac{\partial\varepsilon(t)}{\partial t}\right], \quad \tau = \frac{\eta}{E}. \tag{3.22}$$

Figure 3.4 Front suspension of a classic Vespa scooter showing a shock absorber and a spring in a coilover configuration ("coil spring over shock") to the left. The structure to the right is a swing-arm. Image: Public domain, from Wikipedia Commons. (Wikipedia)

The model is named after William Thomson (Baron Kelvin) and Woldemar Voigt. The suspension system of Fig. 3.4 where the spring and the damper are in parallel can be recognized as the Kelvin-Voigt model. The constitutive equation in the frequency domain is given in (3.19).

The derivation and the properties of the solution are given in [Holm, 2019b, Chap. 2.4]. The main characteristics is that when $\omega\tau \ll 1$, attenuation increases with ω^2 and phase velocity is approximately constant and equal to c_0. However when $\omega\tau \gg 1$, the attenuation and the phase velocity will increase with $\sqrt{\omega}$ and the phase velocity will therefore increase without limits.

☞ Quadratic attenuation is the first order approximation for attenuation in air and seawater

[1] The link to earlier notation in these notes is that stress $\sigma = -p$, and strain $\varepsilon \approx -\rho/\rho_0$ [Holm, 2019b, App. B.1.1].

3.3.2 Derivation from the Navier-Stokes equation

[Landau and Lifshitz, 1987] show that Euler's equation can be generalized to the Navier-Stokes equation to include viscosity:

$$\rho_0 \frac{\mathrm{D}\vec{v}}{\mathrm{D}t} = \rho_0 \left(\frac{\partial \vec{v}}{\partial t} + \vec{v} \cdot \nabla \vec{v} \right) = -\nabla p + \eta \nabla^2 \vec{v} + (\zeta_B + \frac{1}{3}\eta) \nabla (\nabla \cdot \vec{v}), \tag{3.23}$$

where the two coefficients of viscosity are η, the shear viscosity and ζ_B, the bulk viscosity. This equation has two more terms on the right-hand side compared to (2.3).

The Navier-Stokes equation is simplified in the case of an incompressible fluid, where $\nabla \cdot \vec{v} = 0$:

$$\rho_0 \frac{\mathrm{D}\vec{v}}{\mathrm{D}t} = \rho_0 \left(\frac{\partial \vec{v}}{\partial t} + \vec{v} \cdot \nabla \vec{v} \right) = -\nabla p + \eta \nabla^2 \vec{v}. \tag{3.24}$$

In that case it is only the shear viscosity which matters.

It is shown in [Holm, 2019b, App. B.1,1] how this is equivalent to the spring-damper model of (3.22) and therefore leads to the same viscous wave equation.

3.4 The relaxation wave equation

The problem with the asymptotically infinite phase velocity and the impulse in the relaxation modulus of the Kelvin-Voigt model is due to a breakdown of the continuity assumption, i.e. wavelengths approach molecular dimensions. This is the microscale perspective. From a macroscale perspective, the Zener model can be regarded as a more accurate model of the suspension system of Fig. 3.4 if one assumes that the connecting rods of the shock absorber are not perfectly stiff but exhibit some elasticity. It is therefore often a more realistic model. This leads to the standard linear solid model or the Zener model named after Clarence M. Zener. Its constitutive equation is:

$$\sigma(t) + \tau_\sigma \frac{\partial \sigma(t)}{\partial t} = E_e \left[\varepsilon(t) + \tau_\varepsilon \frac{\partial \varepsilon(t)}{\partial t} \right]. \tag{3.25}$$

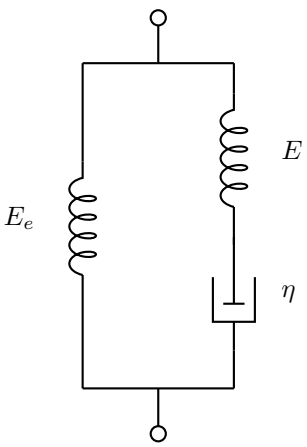

Figure 3.5 Zener or Standard Linear Solid constitutive model

The spring damper arrangement in Fig. 3.5 is one of two ways of representing a standard linear solid model, see [Holm, 2019b, Chap. 3]. Despite that name it is important for the acoustics of fluids as well. Media like salt water and air may be considered as solids as long as the model only deals with perturbations of stress and strain. Therefore the standard linear solid also applies to the acoustics of gases and liquids and it is in fact the building block of the relaxation model which is at the core of the salt water and air attenuation models.

The relaxation and retardation times, τ_σ and τ_ε in (3.25), are the time constants of the temporal step responses. The parameters of the model relate to the physical parameters in Fig. 3.5:

$$\tau_\sigma = \eta / E \leq \tau_\varepsilon = \eta / E', \quad \frac{1}{E'} = \frac{1}{E_e} + \frac{1}{E}. \tag{3.26}$$

The Zener model is one of the standard models in linear viscoelasticity and [Tschoegl, 1989] groups it along with other models with minimum number of elements. In this lies the implication that models with only two parameters, such as the Kelvin-Voigt model, are too elementary to model realistic materials and that these simple models are just building blocks for the more complex ones.

3.4.1 Zener model wave equation

The Zener model's constitutive relation is found by Fourier transforming (3.25) leading to a dynamic modulus which is:

$$\tilde{E}(\omega) = E_e \frac{1 + \mathrm{i}\omega\tau_\varepsilon}{1 + \mathrm{i}\omega\tau_\sigma}, \quad \omega \neq 0. \tag{3.27}$$

Insertion in (3.10) leads to the following wave equation given in [Holm and Näsholm, 2011]:

$$\nabla^2 \vec{u} - \frac{1}{c_0^2}\frac{\partial^2 \vec{u}}{\partial t^2} + \tau_\varepsilon \frac{\partial}{\partial t}\nabla^2 \vec{u} - \frac{\tau_\sigma}{c_0^2}\frac{\partial^3 \vec{u}}{\partial t^3} = 0, \tag{3.28}$$

which has an additional loss term compared to that of the viscous wave equation. The new term ensures a finite phase velocity even in the limit as frequency approaches infinity. The extra loss term is proportional to τ_σ and if that time constant is set to zero both the constitutive equation and the wave equation reduce to the viscous case.

The derivation of the wave equation and its properties are discussed in [Holm, 2019b, Chap. 2.5-2.6]. Those sections also discuss how sums of relaxation models are at the core of the attenuation models for common media.

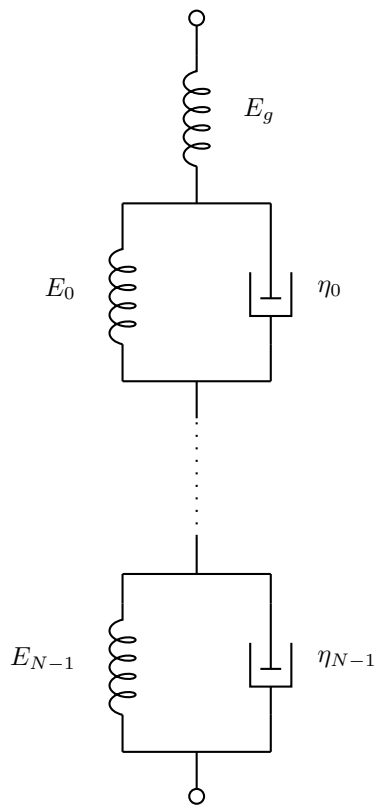

Figure 3.6 The generalized Kelvin-Voigt or Kelvin model

3.4.2 Multiple relaxation

The multiple relaxation model assumes multiple sections consisting of a spring in series with N parallel combinations of springs and dampers as shown in Fig. 3.6. In general this will result in a very complicated result for the attenuation with cross coupling between the terms. Usually the time constants of the model, (3.26), are very close to each other also, $\tau_\sigma \lesssim \tau_\varepsilon$. This is stricter than (3.26).

It is shown in [Holm, 2019b, 2.6.2] that often the individual contributions to the attenuation and sound velocity can be added directly:

$$\alpha_k(\omega) = \sum_{n=0}^{N-1} \frac{A_n \omega_n}{\omega^2 + \omega_n^2}\omega^2, \tag{3.29}$$

Each term contributes an attenuation which increases with ω^2 at low frequencies and a constant value above the relaxation frequency, ω_n. The relaxation frequency is $\omega_n = 1/\tau_\varepsilon$ in each underlying Zener model. The constants A_n are given by the parameters of the model in Fig. 3.6.

In acoustics, the first term is often a simple quadratic term rather than a relaxation term. In order to arrive at that formula, let the first relaxation

frequency be much larger than the highest frequency of interest, i.e. $\omega_0 \gg \omega_n, n = 1 \ldots N$ or let the damper, η_0, in branch 0 be much smaller than the others. Then the first term may be simplified. It is often then called a viscous term. The common way of writing multiple relaxation is the result:

$$\alpha_k(\omega) = A_0\omega^2 + \sum_{n=1}^{N-1} \frac{A_n\omega_n}{\omega^2 + \omega_n^2}\omega^2. \tag{3.30}$$

The phase velocity also consists of individual decoupled term, with their inverses summed:

$$\frac{1}{c_{ph}(\omega)} = \frac{1}{c_0} - \sum_{n=1}^{N-1} \frac{A_n\omega^2}{\omega^2 + \omega_n^2}. \tag{3.31}$$

3.5 Attenuation in typical media

Both seawater and air have an attenuation which is usually modeled with three terms in the expressions above.

3.5.1 Seawater

In salt water, the most abundant substance is sodium chloride or $NaCl$. Somewhat surprisingly $NaCl$ does not contribute to attenuation. Instead the two important relaxation processes are due to magnesium sulfate, $MgSO_4$, up to a few 100 kHz, and boric acid, $B(OH)_3$ or H_3BO_3, up to a few kHz. Magnesium sulfate relaxation is due to a perturbation in the balance between $MgSO_4$ and Mg^{++}, SO_4^{--}:

$$\mathrm{MgSO_4} \rightleftharpoons \mathrm{Mg^{++}} + \mathrm{SO_4^{--}} \tag{3.32}$$

Typical curves for attenuation in seawater are shown in Fig. 3.7 with different curves for representative parameter sets for the major oceans of the world [Ainslie and McColm, 1998]. One can recognize how each of the curves is made up of two relaxation contributions overlaid on a curve for distilled water which is proportional to f^2, i.e. the low frequency part of the viscous wave solution.

Fast sound in water

Water has an intriguing property in that the phase velocity increases to about 3200 m/s, close to the value for ice, at extremely high frequencies. This effect was first predicted from molecular dynamics simulations in 1974 and measured by inelastic neutron scattering in 1985. The effect takes place at wavenumbers higher than 1 nm^{-1}, i.e. wavelengths smaller than about 6 nm. This is only about 20 times the length between oxygen molecules in the hydrogen bond of water, so one is close to the molecular scale.

Several theories have been advanced to explain it, but the most likely one seems to be that it is based on structural relaxation [Santucci et al., 2006]. Such a relaxation model predicts an elevated high frequency phase velocity, (3.31). This confirms that all the terms in the attenuation model for seawater are relaxation terms, i.e. that (3.29) is the correct model and that (3.30) is an approximation.

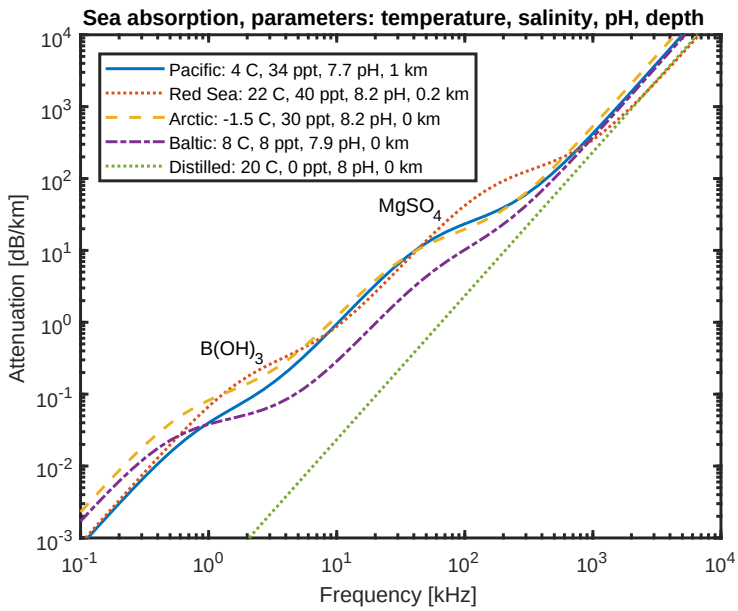

Figure 3.7 Attenuation in seawater for various oceans of the world, parameters from [Ainslie and McColm, 1998]

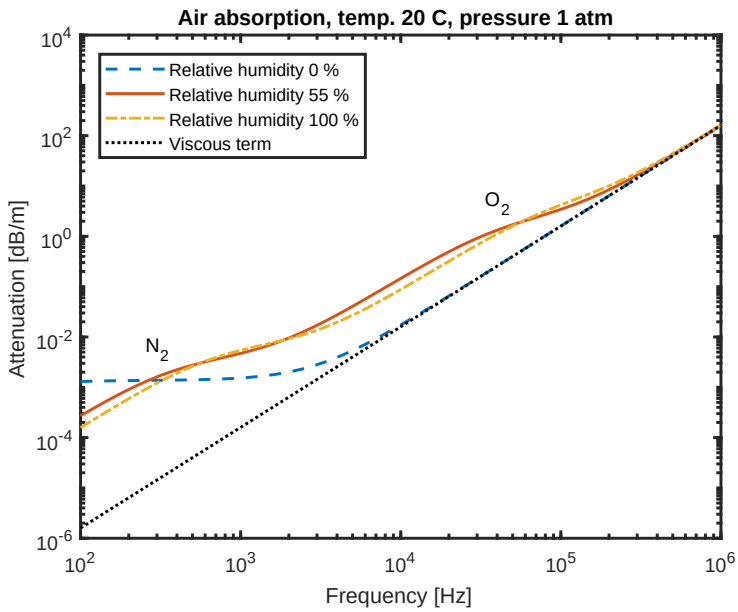

Figure 3.8 Attenuation in air at temperature 20°C and for 0%, 55%, and 100% relative humidity. The lower curve is the contribution due to viscosity and heat conduction alone

3.5.2 Air

In air one usually considers two thermal relaxation processes in addition to a viscous process. The relaxation processes are due to nitrogen, N_2 and oxygen, O_2 and their interaction with water vapor. Nitrogen has a relaxation frequency in the low kHz range, and for oxygen it is in the 10-100 kHz range [Bass et al., 1972, Evans et al., 1972].

Attenuation in air is shown in Fig. (3.8) at temperature 20°C with humidity as a parameter. The attenuation starts to become significant above about 10 kHz. Therefore attenuation for audible frequencies, especially those which are important for speech (up to 8-10 kHz), is usually neglected unless one is concerned with the propagation of noise over large distances as for instance is the case around airports or highways.

In some professional audio system for use outdoors it is also possible to correct for it. The value at 10 kHz can reach 0.1 dB/m, and as it increases approximately with frequency squared, it may reach 2-3 dB/m at 100 kHz. That means that it must be taken into consideration for positioning and communications systems at ultrasonic frequencies, such as systems operating in the 40 kHz range [Holm et al., 2005, Holm, 2012].

Chapter 4

Power-law attenuation and complex media

In several media, attenuation is very different from that described by the classical models described so far. Examples can be found in wave propagation of both shear and pressure waves in sub-bottom sediments, in rocks (seismics), and in medical ultrasound imaging [Szabo and Wu, 2000]. Possibly the first suggestion to use fractional derivatives to model such frequency dependent viscoelasticity was in [Gemant, 1936] to fractional powers in the frequency domain.

As an example, a common rule-of-thumb for design of ultrasound systems is that attenuation varies linearly with frequency with attenuation equal to 0.5 dB/MHz/cm. That means that $y = 1$ and $\alpha_0 = 0.5/(2\pi \cdot 8.686)$ Np/radian frequency-cm in

☞ A first order approximation is that attenuation varies linearly with frequency in medical ultrasound

$$\alpha_k = \alpha_0 |\omega|^y, \quad 0 \le y \le 2. \tag{4.1}$$

A comparison between the typical or "rule-of-thumb" attenuation' of tissue and the absorption of seawater from Fig. 3.7 is shown in Fig. 4.1. The figure also shows attenuation from a range of different tissue types from blood as the lowest with 0.14 dB/cm/MHz and $y = 1.21$ to breast with 0.75 dB/cm/MHz and $y = 1.5$ [Duck, 2012], [Szabo, 2014, App. B]. Milk happens to have the same characteristics as the "rule-of-thumb attenuation". This figure should make it clear that attenuation in tissue is very different from that of water. First of all it is much higher and second it has a different frequency dependency.

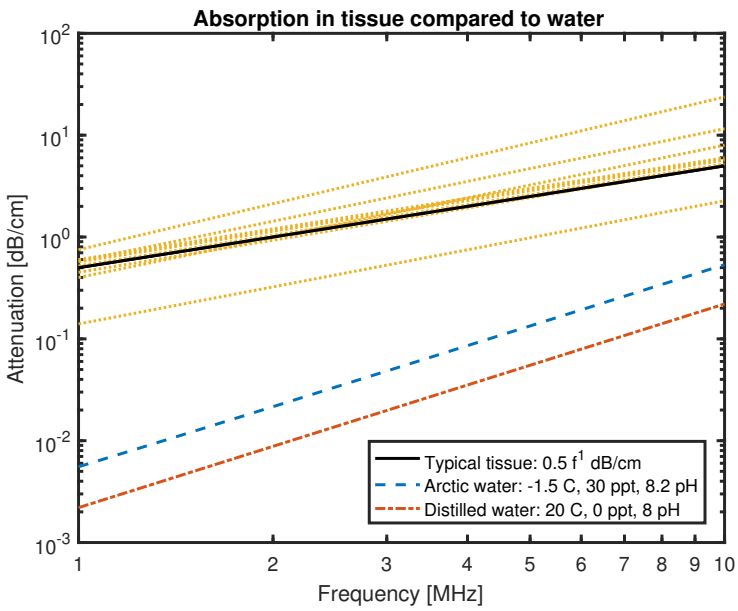

Figure 4.1 Absorption in typical tissue as well as for a representative selection of tissue types compared to the highest and lowest attenuation in water from 1 to 10 MHz

It should also be noted that fluids without the solid matrix of tissue, such as milk and blood, have similar attenuation as tissue. This is supported by [Carstensen et al., 1953] which concluded that the absorption of blood is directly proportional to protein concentration. Thus the solid matrix seems to contribute little to the attenuation of the compressional wave.

4.1 Modeling with multiple relaxation processes

It is possible to model almost arbitrary power-law attenuation over a limited frequency range by adding up several carefully selected relaxation processes as in Sec. 4.1. This can be seen in e.g. Fig. 3.7. Although the general trend in this figure is that attenuation increases with $y = 2$ with reference to (4.1), it is easy to see some frequencies where attenuation increases with a smaller values of y closer to 1 also.

A method for selecting relaxation parameters based on the desired power-law and frequency range based on [Näsholm, 2013]. Let the contributions from individual relaxation processes add as in (3.29):

$$\alpha_k(\omega) = \sum_{n=0}^{N-1} \frac{A_n \omega_n}{\omega^2 + \omega_n^2} \omega^2. \tag{4.2}$$

When it is desired to model an attenuation that increases as ω^y, it can be shown that the weights, when the relaxation frequencies are spread evenly on a log scale, $\omega_{n+1}/\omega_n = C$, should be:

$$A_n \propto \omega_n^\alpha, \quad \alpha = y - 1, \tag{4.3}$$

where α is the order of the equivalent fractional model of the next section.

In Fig. 4.2 an example from [Holm, 2019b, Sect. 7.2] is given where $y = 1.3$, $N = 5$, and $\omega_{n+1}/\omega_n = 4$. Notice how well the approximation follows the desired curve over several decades of frequency, approximately over the range spanned by the five values of ω_n as indicated by the five stars in the figure. If a power law with $y = 1$ had been desired, it would have meant that all the weights should have the particularly simple value of unity, $A_n = 1$.

When the processes are fitted to data to achieve a certain power law, the parameters of the model usually no longer have any physical significance as in the seawater and air models. Despite this, the multiple relaxation processes involved may take their inspiration from hierarchical structures as for instance in the collagen of tendons, ligaments, and skin where one can identify five substructures: Collagen molecule, collagen fibril, fibril bundle, fascicle, and whole tendon. This may explain a power-law response over 3-4 decades of frequency [Shen et al., 2011]. Likewise, a cell is hierarchical and consists of the cell membrane, cortex (a thin actin network under the membrane), and the cytoskeleton [Broedersz and MacKintosh, 2014].

However, in cell biomechanics, [Kollmannsberger and Fabry, 2011] argue that there are just too few cell components in a hierarchy from the largest to the smallest mechanical structure to account for an observed five decades of power-law behavior. They argue instead for power-law models based on a theory of soft glassy materials and say the following:

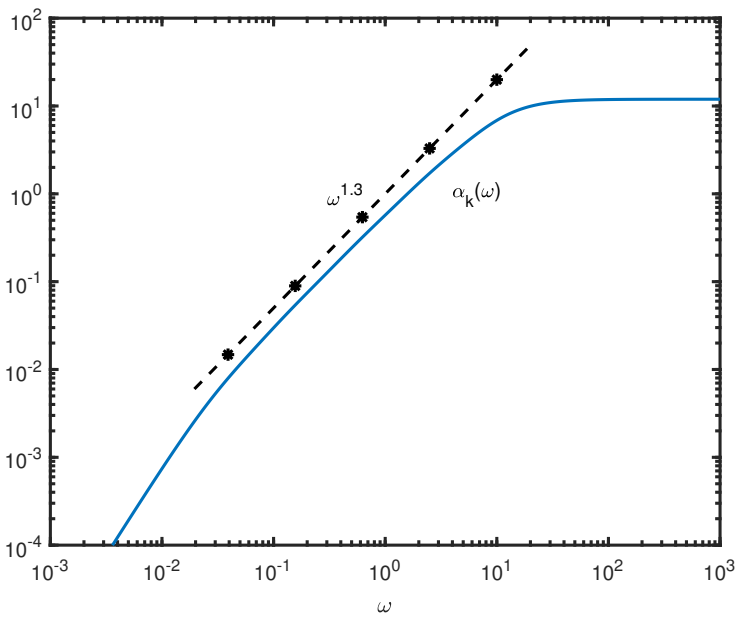

Figure 4.2 Multiple relaxation approximation to power-law attenuation with slope $y = 1.3$. Solid curve: superposition of five relaxation processes. Dot-dashed curve: $\omega^{1.3}$, the five relaxation frequencies are indicated by stars

> "It has been noted that generic concepts of soft glassy rheology lend themselves straightforwardly to an interpretation of power-law cell behavior. Accordingly, the cell is imagined to consist of many disordered elements held in place by attractive or repulsive bonds, traps, or energy wells formed between neighboring elements. The binding energies are weak enough to allow the elements to occasionally hop out of their trap and change their position. Power-law rheology arises from a wide distribution of energy well depths such that the distribution of element lifetimes is scale-free."

The link between complex media parameters and the relaxation parameters is an open area of research and it is unknown, except for the mathematics, why a simple relationship like (4.3) is so successful in capturing power-law behavior. Answers to such questions could also shed light on why the fractional model of the next section is so successful in describing complex systems.

4.2 Fractional models

In this section the goal is to find a wave equation that has realistic power-law attenuation for complex media with exponent y close to 1.

4.2.1 Convolution loss operator

In order to generalize a lossy wave equation, one may replace the loss term by a convolution with some kernel $\Psi(t)$:

$$\nabla^2 u - \frac{1}{c_0^2}\frac{\partial^2 u}{\partial t^2} + \Psi(t) * u = 0. \tag{4.4}$$

Example 4.1 Operators of viscous and relaxation wave equations.

The Zener model's wave equation, i.e. that of the relaxation mechanism of (3.28) corresponds to this operator:

$$\Psi(t) * u = \tau_\varepsilon \frac{\partial}{\partial t}\nabla^2 u - \frac{\tau_\sigma}{c_0^2}\frac{\partial^3 u}{\partial t^3}. \tag{4.5}$$

Only the first term is required for the viscous wave equation of (3.21).

Taking a clue from the viscous loss operator, we will restrict the kernel to those that include a Laplacian in what follows. The new kernel, $\Phi(t)$ is related to the old one as follows: $\Psi(t) * u = \Phi(t) * \nabla^2 u$.

Compared to (3.21), the first order temporal derivative has now been replaced by a convolution with a kernel $\Phi(t)$:

$$\nabla^2 u - \frac{1}{c_0^2}\frac{\partial^2 u}{\partial t^2} + \Phi(t) * \nabla^2 u = 0. \tag{4.6}$$

How can $\Phi(t)$ be selected to fit measurements? A temporal power law convolved with an m'th order derivative will turn out to be a good choice. In what follows, the integer $m = \lceil \alpha \rceil$, i.e it is the smallest integer larger than α:

$$\Phi(t) * f(t) = \tau^\alpha \frac{\mathrm{d}^m f(t)}{\mathrm{d}t^m} * \frac{1}{\Gamma(m-\alpha)\, t^{\alpha+1-m}}, \quad 0 < \alpha \le 1, \tag{4.7}$$

where $\Gamma(\cdot)$ is the gamma function, a generalization of the factorial function to non-integers as $\Gamma(n) = (n-1)!$ for integer n.

The reason why the temporal power-law kernel is desirable is because its Fourier transform is also a power law:[1]

$$F\Big(\frac{\mathrm{d}^m f(t)}{\mathrm{d}t^m} * \frac{1}{\Gamma(m-\alpha)\, t^{\alpha+1-m}}\Big) = (\mathrm{i}\omega)^\alpha F(\omega). \tag{4.8}$$

The memory kernel consisting of the temporal power law scaled by the gamma function of (4.7), sometimes called the Abel kernel, is illustrated in Fig. 4.3 with $m = 1$ and α as parameter. Its interpretation is:

- As α approaches 1 the operator is supposed to turn into a first order derivative. This can be seen by letting $\alpha = 1 - \varepsilon^+ < 1$ and as $\Gamma(\varepsilon^+) \to \infty$

[1] See https://proofwiki.org/wiki/Laplace_Transform_of_Power

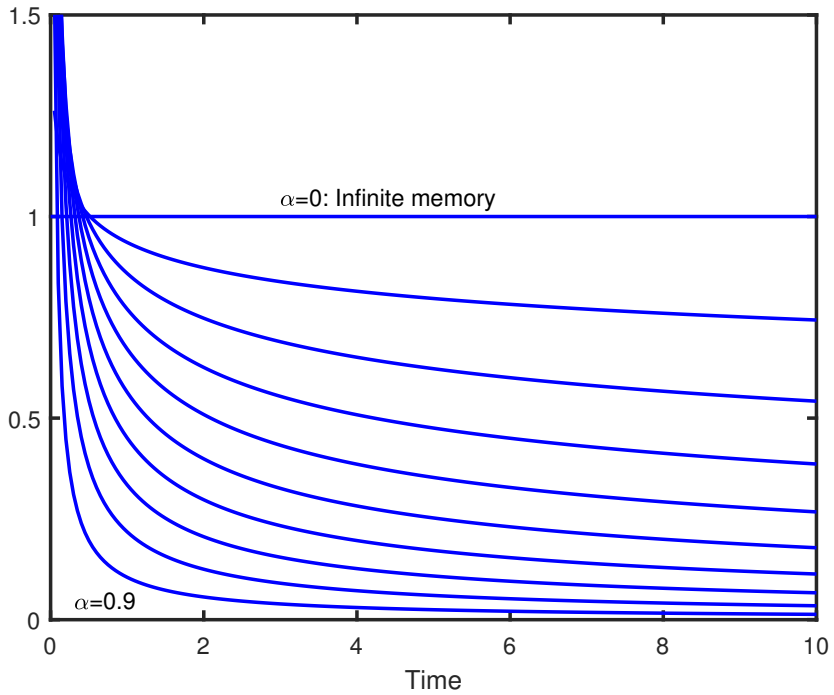

Figure 4.3 A plot of the power-law memory kernel in the convolution function of (4.7) for $m = 1$. The curves illustrate values of α from 1 in the upper curve to 0.1 in the lower curve in increments of 0.1 (inspired by [Treeby and Cox, 2010])

for $\varepsilon^+ \to 0$, the memory kernel approaches an impulse and the memory is gone. As a test, let's try to insert $m = \alpha = 1$ in (4.7):

$$\Phi(t) * f(t) = \lim_{\alpha \to 1} \frac{\mathrm{d} f(t)}{\mathrm{d} t^m} * \frac{1}{\Gamma(1-\alpha)\, t^\alpha} = \tau \frac{\mathrm{d} f(t)}{\mathrm{d} t} * \delta(0) = \tau \frac{\mathrm{d} f(t)}{\mathrm{d} t}, \quad (4.9)$$

where $\delta(t)$ is the impulse function. This gives us the loss operator of the viscous wave equation as desired.

- As α approaches 0, the kernel turns into an ordinary integral, i.e. one with infinite memory and the differentiation is canceled.

4.2.2 Fractional or non-integer order derivative

The former expression, (4.8), is reminiscent of the differentiation property of the Fourier transform:

$$F\Big(\frac{\mathrm{d}^m f(t)}{\mathrm{d} t^m}\Big) = (\mathrm{i}\omega)^m F(\omega). \quad (4.10)$$

In fact, (4.8) is one common way that a non-integer or fractional derivative can be defined. That means that the general loss kernel of (4.6) is in fact a derivative of arbitrary order, often called a fractional derivative:

$$\Phi(t) * f(t) = \tau^\alpha \frac{\mathrm{d}^m f(t)}{\mathrm{d} t^m} * \frac{1}{\Gamma(m-\alpha)\, t^{\alpha+1-m}} = \tau^\alpha \frac{\mathrm{d}^\alpha f(t)}{\mathrm{d} t^\alpha} \quad (4.11)$$

Riemann-Liouville and Caputo fractional derivatives

For the purpose of these lecture notes, the frequency domain definition of (4.8) is the only definition which is needed. If a fractional derivative is needed in a numerical evaluation, one will also need the time domain expression. Its most important property is that it has a long-tailed power-law memory which is a challenge computation-wise.

The convolution above can be written in two different ways, depending on the order of the operations. First, for terminology, the general expression for the fractional derivative of order α is written as:

$$\frac{\mathrm{d}^\alpha f(t)}{\mathrm{d}t^\alpha} = {}_a\mathrm{D}_t^\alpha f(t), \tag{4.12}$$

where a and t are limits in the defining integral. If the order is negative, $\alpha < 0$, this is a fractional integration.

The Riemann-Liouville fractional derivative of order $\alpha \in R$, $m-1 \leq \alpha < m$ is:

$${}_a\mathrm{D}_t^\alpha f(t) = \frac{1}{\Gamma(m-\alpha)}\left(\frac{\mathrm{d}}{\mathrm{d}t}\right)^m \int_a^t \frac{f(t')}{(t-t')^{\alpha+1-m}}\mathrm{d}t' \tag{4.13}$$

Here the convolution operation of (4.11) is the first operation to be performed followed by the integer order derivation. It was first given in [Liouville, 1832].

The order of operations is reversed in the Caputo fractional derivative [Caputo, 1967]:

$${}_a^C D_t^\alpha f(t) = \frac{1}{\Gamma(m-\alpha)} \int_a^t \frac{f^{(m)}(t')}{(t-t')^{\alpha+1-m}}\mathrm{d}t', \tag{4.14}$$

where $f^{(m)}(t)$ is the m'th order derivative. First an integer order derivative of order m is performed, and then a convolution with the power-law memory kernel takes place. This definition of a fractional derivative was first given in [Abel, 1823] as was recently discovered, [Podlubny et al., 2017].

When the function is a constant, the first integer order derivative in the Caputo definition will ensure that the result is zero, thus giving the expected result of 0, opposite to what the Riemann-Liouville derivative does. In addition to the different handling of constants, the difference between the two becomes evident whenever numerical time domain implementations are required. The Riemann-Liouville derivative turns out to require initialization of derivatives of non-integer orders. This is different for the Caputo fractional derivative which will require initialization of integer order derivatives: $f^{(k)}(0), k = 0, 1, \ldots, m-1$. They are the ones that usually have physical meaning and therefore the Caputo definition is often simpler to use in numerical implementations.

The fact that different definitions of the fractional derivative may give different results could explain why it has taken a long time for the fractional derivative to be accepted.

Power-law material responses

The convolution with a temporal power law in (4.13) and (4.14) means that the material responses imply a temporal memory. A fractional derivative is

therefore a global operator which takes all of the time history of the function into account. This is in contrast to integer order derivatives which are local as it is only the slope, curvature, etc at the time instant in question which matters.

The implication of the Fourier relation of (4.8) is that in the medical and geophysical applications mentioned previously where power-law attenuation is prevalent, it is possible to find temporal power-law responses or related responses such as the Mittag-Leffler function. The Mittag-Leffler function is a parameterized function with an exponential-like behavior for small arguments and a power-law tail for large arguments.[2] It also means that observations in diverse materials of temporal power laws similar to (4.7) that go back to [Nutting, 1921, Blair and Reiner, 1951], result in power laws in the frequency domain.

4.2.3 Fractional wave equations

The theory of fractional calculus may be applied to medium models similar to (3.22) and (3.25) by letting the derivatives be generalized to fractional derivatives. That leads to fractional derivatives in the wave equations, such as (3.21) and (3.28).

As an example, the fractional Zener model is:

$$\sigma(t) + \tau_\sigma^\alpha \frac{\partial^\alpha \sigma(t)}{\partial t^\alpha} = E\left[\varepsilon(t) + \tau_\varepsilon^\alpha \frac{\partial^\alpha \varepsilon(t)}{\partial t^\alpha}\right], \quad 0 < \alpha \le 1. \tag{4.15}$$

It leads to

$$\nabla^2 \vec{u} - \frac{1}{c_0^2}\frac{\partial^2 \vec{u}}{\partial t^2} + \tau_\varepsilon^\alpha \frac{\partial^\alpha}{\partial t^\alpha}\nabla^2 \vec{u} - \frac{\tau_\sigma^\alpha}{c_0^2}\frac{\partial^{\alpha+2}\vec{u}}{\partial t^{\alpha+2}} = 0. \tag{4.16}$$

Its attenuation, when time constants are almost similar as in Sec. 4.1, is

$$\alpha_k(\omega) \propto \frac{\omega_n}{\omega^{2\alpha} + 2\omega^\alpha \omega_n^\alpha \cos\frac{\pi\alpha}{2} + \omega_n^2}\omega^{1+\alpha} \propto \begin{cases} \omega^{1+\alpha}. & \omega \ll \omega_n \\ \omega^{1-\alpha}, & \omega \gg \omega_n, \end{cases} \tag{4.17}$$

which is a generalization of each of the terms of the relaxation sum of (3.29). If for instance the parameter α is slightly larger than 0, attenuation which increases near proportional to frequency can be achieved, as is desired in applications in medical ultrasound and sediment acoustics.

The fractional Zener model also describes other media such as dielectrics, as it is equivalent to a Cole-Cole medium [Holm, 2020].

The Grain Shearing model for sediment acoustics, [Buckingham, 2000], is in fact a fractional model with a fractional Kelvin-Voigt model for the compressional wave, i.e. $\tau_\sigma = 0$ in (4.16) and a fractional diffusion-wave equation for the shear wave [Pandey and Holm, 2016]. The latter is

$$\nabla^2 \vec{u} - \frac{\rho_0}{\eta}\frac{\partial^{2-\alpha}\vec{u}}{\partial t^{2-\alpha}} = 0, \tag{4.18}$$

[2] See https://en.wikipedia.org/wiki/Mittag-Leffler_function

where ρ_0 is density and η viscosity. Changing the fractional order allows interpolation from a diffusion equation which describes for instance heat propagation for $\alpha = 1$ to a lossless wave equation for $\alpha = 0$. Typical values in sediment acoustics are α just slightly above 0. This kind of connection between physics and mathematics was recently listed as one of several contributions to *developing models with physical and mathematical rigor that led to an f^1 dependence which was, until recently, but an empirical supposition*, to quote [Holland and Dosso, 2022].

The Viscous Grain Shearing model for sediment acoustics, [Buckingham, 2007], is slightly more complicated than the Grain Shearing model as it has a low-frequency response that better fits data (proportional to ω^2). It is also a fractional model with a more complicated kernel. This analogy is developed in [Holm et al., 2023, Chandrasekaran et al., 2023].

The derivation of wave equations like those above, their properties, and how they suit complex media better than the classical equations, is the main topic of the book [Holm, 2019b].

Chapter 5

Nonlinear acoustics

Acoustic waves exhibit nonlinearity both in water, air, and in tissue. Like ocean waves, as shown in Fig. 5.1, this will lead to a distortion of a sinusoidal and steepening of the wave form. Unlike ocean waves however, acoustic waves are not surface waves, and therefore cannot break as the image shows.

Important applications of nonlinear acoustics are in harmonic imaging in ultrasound and in parametric sonar:

- Harmonic imaging is where an ultrasound scanner receives the scattered signal at twice the transmitted frequency, based on nonlinearity in the medium which leads to harmonic distortion. In many scanners today it is the default mode.

- Parametric sonar utilizes intermodulation distortion in the medium between two transmitted frequencies. Often the difference frequency is utilized because a parametric echo sounder can produce it with much smaller source dimensions than if it had been generated directly. This is important for low-frequency echo sounders for use in sub-bottom profiling. The principle can also be used in air in order to produce highly directional audio sources.

Figure 5.1 The great wave off Kanagawa (Wikipedia). Katsushika Hokusai c. 1830 , Public Domain, via Wikimedia Commons.

There are three potential sources of nonlinearity:

- The equation of continuity (mass conservation law), (2.5)

- Euler's equation (conservation of momentum), (2.3)

- The constitutive law, (2.8)

Since nonlinearity is a level dependent effect, conversion between sound pressure levels in air and water is also included in this chapter.

5.1 Nonlinearity in the conservation laws

In practice, weak nonlinearity is what is encountered in the applications just mentioned. It then turns out that the nonlinearity in the conservation of momentum equation can be neglected. Only the nonlinearity due to the gradient of the density in (2.5), the equation of continuity, will contribute. This term accounts for a convective nonlinearity where the particle velocity contributes to the wave velocity [Hamilton and Blackstock, 1988]. The consequence is that the movement of molecules in the fluid will have a propagation velocity which is $c = c_0 + u(t)$ due to the particle velocity, $u(t)$, even if the material's constitutive equation is perfectly linear.

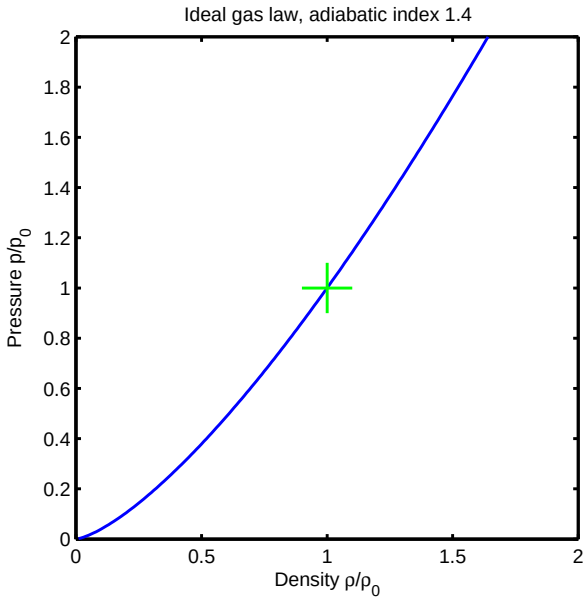

Figure 5.2 Gas law for an adiabatic process (no transfer of heat or matter to and from the surroundings) with $\gamma = 1.4$ showing the 1 atmosphere point around which linearization takes place

5.2 Nonlinear constitutive equation

5.2.1 Acoustics of an ideal gas

The constitutive law or the equation of state comes from the ideal gas equation, $pV^\gamma = C$ of (2.8), where γ is the adiabatic gas constant or heat capacity ratio, $\gamma = c_p/c_v$.[1] In an ideal gas, where the space taken up by the molecules can be neglected their is no interaction between molecules, $\gamma = 1.4$. This is a reasonable approximation for air.

Since the density is inverse proportional to volume, V, the gas law can be rewritten as:

$$\frac{p}{p_0} = \left(\frac{\rho}{\rho_0}\right)^\gamma \tag{5.1}$$

where p_0, ρ_0 are the static values. It is plotted in Fig. 5.2.

The Taylor series for the pressure variation is:

$$p - p_0 = A\frac{\rho - \rho_0}{\rho_0} + \frac{B}{2!}\left(\frac{\rho - \rho_0}{\rho_0}\right)^2 + \cdots, \tag{5.2}$$

where $A = p_0\gamma$, $B = p_0\gamma(\gamma - 1)$ and the **nonlinearity parameter** $B/A = \gamma - 1$ which is 0.4 for an ideal gas.

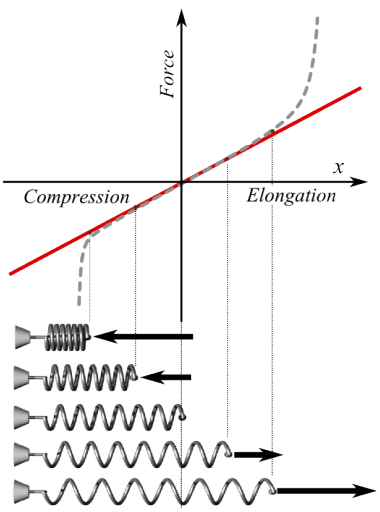

Figure 5.3 Applied force F vs. elongation X for a helical spring according to Hooke's law (red line) and what the actual plot might look like (dashed line) (Wikipedia). By Svjo (Own work) [CC BY-SA 3.0], via Wikimedia Commons.

5.2.2 Elastic waves

For a solid, Hooke's law is a linearization of typical curves as shown in Fig. 5.3.

[1] https://en.wikipedia.org/wiki/Heat_capacity_ratio

5.3 Westervelt equation

Combining the effects due to nonlinearities in the constitutive law and in the conservation equations with the appropriate approximations for weak nonlinearity, leads to this wave equation:

$$\nabla^2 p - \frac{1}{c_0^2}\frac{\partial^2 p}{\partial t^2} + \frac{\delta}{c_0^2}\frac{\partial}{\partial t}\nabla^2 p = -\frac{\beta}{\rho_0 c_0^4}\frac{\partial^2 p^2}{\partial t^2} \tag{5.3}$$

The left-hand part can be recognized as belonging to the viscous wave equation while the right-hand term contains the nonlinearity. Here the **nonlinearity coefficient** is $\beta = 1 + \frac{B}{2A}$.

The loss term has two contributions:

$$\delta = \delta_{me} + \delta_{th} = \frac{1}{\rho_0}\left(\zeta + \frac{4}{3}\eta\right) + \frac{\kappa}{\rho_0}\left(\frac{1}{c_v} - \frac{1}{c_p}\right), \tag{5.4}$$

where ζ is the bulk viscosity, η is the shear viscosity, κ is thermal conductivity, and c_v and c_p the specific heat at constant volume and pressure respectively.

The viscous wave equation can be rewritten in an often used form when low losses or low frequencies, i.e. $\omega\tau \ll 1$, where $\tau = \delta/c_0^2$, can be assumed. Then the viscous wave equation of (3.21) reduces to:

$$\nabla^2 u \approx \frac{1}{c_0^2}\frac{\partial^2 u}{\partial t^2}, \tag{5.5}$$

which is inserted back in the loss term of (5.3). The result is the usual form of the Westervelt equation which has only temporal derivatives in the loss term:

$$\nabla^2 p - \frac{1}{c_0^2}\frac{\partial^2 p}{\partial t^2} + \frac{\delta}{c_0^4}\frac{\partial^3 p}{\partial t^3} = -\frac{\beta}{\rho_0 c_0^4}\frac{\partial^2 p^2}{\partial t^2} \tag{5.6}$$

It should be noted that it is not possible to set up dispersion relations for the nonlinear wave equations. The description in the form of a dispersion relation assumes that Fourier analysis can be used to describe how the medium modifies the wave, and Fourier analysis assumes a linear time-invariant system. This is clearly not satisfied when the medium is nonlinear.

Finally, the speed of sound, c, will vary with particle displacement, u, or pressure p:

$$c(t) = \frac{dx}{dt} = c_0 + (1 + \frac{B}{2A})u(t) = c_0 + (1 + \frac{B}{2A})\frac{p(t)}{\rho_0 c_0} \tag{5.7}$$

showing the link to the claim of item 3 in Chap. 1.

5.3.1 The nonlinearity coefficient and the nonlinearity parameter

The **nonlinearity coefficient**, $\beta = 1 + \frac{B}{2A}$, of (5.3) and (5.6) is the sum of 1 and half the **nonlinearity parameter** B/A. It is interesting to note that even if the constitutive law had been completely linear ($B/A = 0$), there would still be nonlinearity due to the convection term.

In practical media such as water and biomedical tissue, B/A is in the range of 5-10.[2] This is an order of magnitude more than the value predicted for an ideal gas.

[2] https://en.wikipedia.org/wiki/Nonlinear_acoustics

5.4 Sound pressure levels in air and water

In Sec. 3.5, a comparison was made between the attenuation of sound in water and air. It is of interest also to compare Sound Pressure Levels (SPL) in dB between the two media. In water, the SPL often appears to be much higher than in air. It is, however, misleading to compare them directly. This has consequences for understanding important issues in ecology, in particular the impact of humans on marine wildlife, such as whales.

5.4.1 Two conversion steps

Whales regularly emit sound with pressures in excess of 160 dB. Even louder is the small snapping shrimp which may emit 190–210 dB sound pressures. It produces a loud snapping sound by rapid closure of its claw in order to stun or kill its prey [Versluis et al., 2000]. In air, however, a sound level of 120 dB is considered dangerous for humans. The highest airborne sound level that I have been able to find is 165 dB which at 20 kHz proved to be lethal for roaches and caterpillars [Allen et al., 1948].[3]

The numbers are different for two reasons:

1. The reference levels are different. Decibel is the logarithm of a ratio. In air, the reference is the lowest sound a human can hear, and that is a sound pressure of 20 µPa. There is no such natural reference for water, so one has instead chosen a round number, 1 µPa.

2. It is intensity and not pressure which is the fundamental unit that determines the effect of sound or the work it takes to produce it.

The first factor amounts to a dB factor of

$$20\log\frac{20\ \mu\text{Pa}}{1\ \mu\text{Pa}} = 26\ \text{dB} \tag{5.8}$$

The second factor can be understood by considering how a loudspeaker works. In air, with its low density, it requires a large displacement, but quite little force or pressure to generate a sound. Therefore, bass speakers have a displacement of several millimeters and it is often easy to see the motion. In water, it is the other way around, so there will be a lot of pressure for the same work, but very little displacement.

The sound pressure in water can be converted to intensity, and then one has to figure out what pressure that corresponds to in air. Using subscript "a" for air, and "w" for water, the relation is:

$$I = I_a = I_w \Leftrightarrow I = \frac{p_a^2}{\rho_a c_a} = \frac{p_w^2}{\rho_w c_w} \tag{5.9}$$

The equivalent pressure in water is therefore:

$$p_w = \sqrt{I\rho_w c_w} = \sqrt{\frac{\rho_w c_w}{\rho_a c_a}}\,p_a \tag{5.10}$$

[3] These experiments were probably performed prior to the establishment of ethical regulations for animal experiments!

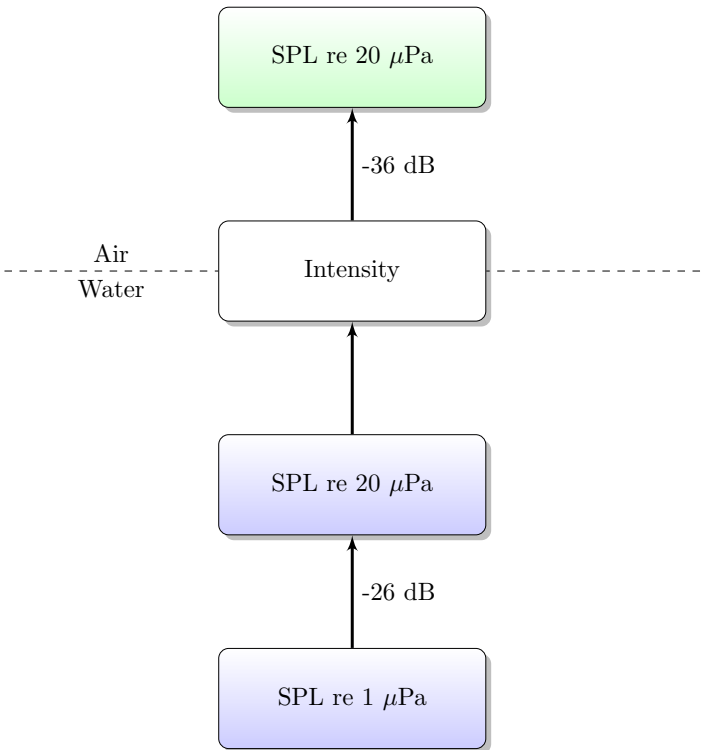

Figure 5.4 The steps to convert from sound pressure in water to that in air (starting in the bottom block)

The net result is that it is the product of density and speed of sound (called acoustic impedance) which is the determining factor. The ratio between the two in water and air is:

$$10\log\frac{\rho_w c_w}{\rho_a c_a} = 10\log\frac{1025\ \mathrm{kg/m^3}\cdot 1500\ \mathrm{m/s}}{1.2\ \mathrm{kg/m^3}\cdot 340\ \mathrm{m/s}} = 35.8\ \mathrm{dB} \approx 36\ \mathrm{dB} \tag{5.11}$$

Adding up the rounded numbers gives a factor of 62 dB. This is the value that must be added to the sound pressure in air to get the equivalent sound pressure in water. The conversion is explained in more detail in [Dahl et al., 2007]. The two steps required to convert from sound pressure in water to that in air are illustrated in Fig. 5.4.

5.4.2 Conversion chart

A chart for conversion is shown in Fig. 5.5, where some typical values for sound pressures are indicated. If you lay a ruler horizontally over the figure, you can read what a sound pressure in air corresponds to in water and vice versa.

It is evident that the whale mentioned initially corresponds to a level in air of 98 dB SPL and the snapping shrimp's lethal level corresponds to about 140 dB SPL in air. Both are still fairly high levels.

There are many examples on the web and in the popular press where the conversion factors of (5.8) and (5.11) are left out giving rise to spectacular claims without any basis in reality.

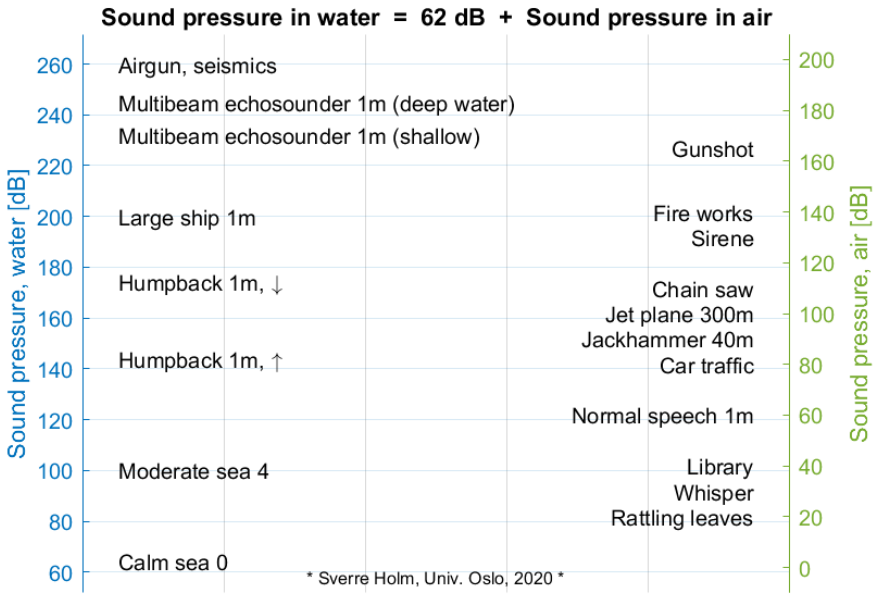

Figure 5.5 Chart for converting between SPL in water and air

Chapter 6

Refraction

This chapter starts by deriving the law of refraction. Then it is applied to typical sound speed profiles in air and seawater. This chapter builds on [Johnson and Dudgeon, 1992, Sect. 2.3].

6.1 Snell's law

The law of refraction can be derived from the condition that the phase should be unchanged on the interface. The component along the interface from the incoming wave should be equal to that of the reflected wave, and to the transmitted wave:

$$\vec{k}_i \cdot \vec{x} = \vec{k}_r \cdot \vec{x} = \vec{k}_t \cdot \vec{x} \tag{6.1}$$

When the interface is along the x-axis as in Fig. 6.1, this becomes:

$$|\vec{k}_1| \cdot \sin\theta_1 = |\vec{k}_r| \cdot \sin\theta_r = |\vec{k}_2| \cdot \sin\theta_2 \tag{6.2}$$

The reflected wave and the incident wave are in the same medium so $|\vec{k}_1| = |\vec{k}_r| = \omega/c_1$ and therefore $\theta_i = \theta_1 = \theta_r$ when θ_r is counted from the normal to the right.

For the refracted wave, the speed of sound/light is different in the two media:

$$\frac{\omega}{c_1} \cdot \sin\theta_i = \frac{\omega}{c_2} \cdot \sin\theta_t \;\Rightarrow\; \frac{\sin\theta_1}{c_1} = \frac{\sin\theta_2}{c_2} \tag{6.3}$$

Snell's law has its name from 1621 after the Dutch astronomer and mathematician Willebrord Snellius (1580-1626). It was described already in 1602 by English Thomas Harriott (1560-1621), but not published [Siegmund-Schultze, 2016]. Later research has brought to light that the law was described already around year 984 by the Persian Abu Said al-Ala Ibn Sahl (940-1000) [Kwan et al., 2002]

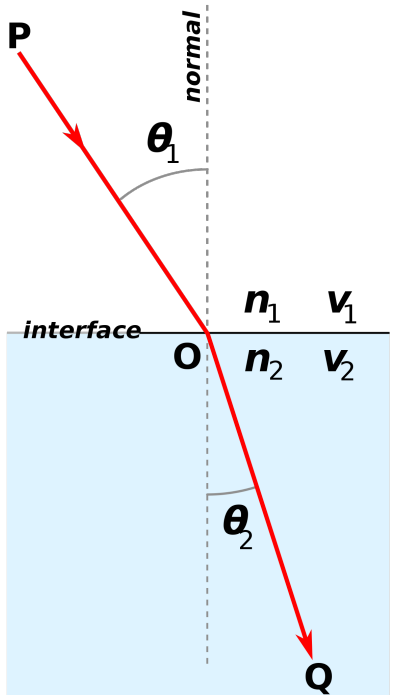

Figure 6.1 Refraction of light at the interface between two media of different refractive indices, with $n_2 > n_1$, where $n = c/c_0$ and c_0 is the vacuum speed. Since the velocity is lower in the second medium ($v_2 = c_2 < v_1 = c_1$), the angle of refraction θ_2 is less than the angle of incidence θ_1; that is, the ray in the higher-index medium is closer to the normal. Wikipedia: https://commons.wikimedia.org/wiki/File:Snells_law2.svg

6.2 Sound speed profiles in typical media

In practical media, there may not be sharp interfaces like in Fig. 6.1, but rather gradual variations so sound speed varies with coordinates as in item 4 in Chap. 1:

$$c = c(x, y, z). \tag{6.4}$$

These media are therefore characterized by sound speed profiles. It is instructive to compute the effect of the simplest sound speed profile, a linear gradient. Here geometrical acoustics is assumed, i.e. an approximate theory which assumes very small acoustic wavelengths, or that medium variations are small over a wavelength.[1]

[1] See https://en.wikipedia.org/wiki/Geometrical_acoustics

Example 6.1 A linear sound speed profile. A wave is propagating horizontally at a depth y_0. Snell's law used on depths y and $y-\delta y$ will be:

$$\frac{\sin\theta(y)}{c(y)} = \frac{\sin\theta(y-\delta y)}{c(y-\delta y).} \tag{6.5}$$

or

$$\frac{\sin\theta(y-\delta y)-\sin\theta(y)}{\sin\theta(y)} = \frac{c(y-\delta y)-c(y)}{c(y)}, \tag{6.6}$$

which in the limit becomes:

$$\frac{1}{\sin\theta(y)}\frac{\mathrm{d}\sin\theta}{\mathrm{d}y} = \frac{1}{c(y)}\frac{\mathrm{d}c}{\mathrm{d}y}. \tag{6.7}$$

Integrate:

$$\ln(\sin\theta) = \ln(c) + C_0 \;\Rightarrow\; \sin\theta(y) = C_1 c(y),\;\; C_1 = \mathrm{e}^{C_0} \tag{6.8}$$

Assume now that sound speed increases linearly with depth, $c(y) = ay$. Further $\sin\theta(y_0) = 1$ from horizontal initial propagation. Inserted in (6.8) this gives a value for C_1, and the solution is:

$$\sin\theta = C_1 c(y))|_{C_1=1/(ay_0)} = \frac{y}{y_0}, \tag{6.9}$$

which describes a circle of radius y_0. The ray will therefore be bent upwards.

☞ Waves always bend towards the slowest medium when there is a gradient in velocity

The following sections on seawater and air have been taken from and expand on [Holm, 2019b, Sect. B.1].

6.2.1 Seawater

In water the bulk modulus is approximately K=2.2 GPa and the density is $\rho_0 = 1000$ kg/m^3 giving $c_0 = 1483$ m/s. Seawater is denser because of the salt and the bulk modulus and density also vary with temperature and other parameters.

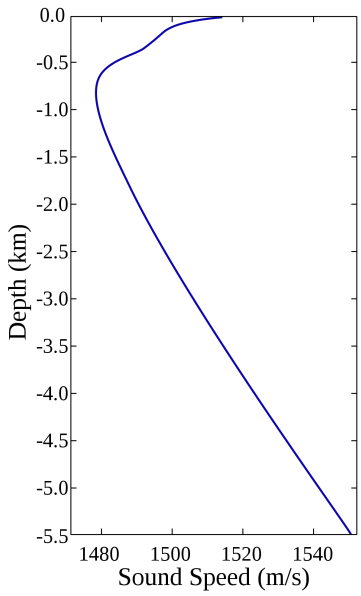

Figure 6.2 Speed of sound as a function of depth at a position north of Hawaii in the Pacific Ocean derived from the 2005 World Ocean Atlas. Wikipedia https://en.wikipedia.org/wiki/Speed_of_sound#/media/File:Underwater_speed_of_sound.svg

Example 6.2 Speed of sound in seawater. An empirical formula for the speed of sound is the nine-term equation of [Mackenzie, 1981]:

$$\begin{aligned} c_0 &= 1448.96 + 4.591T - 5.304\cdot 10^{-2}T^2 + 2.374\cdot 10{-}4T^3 \\ &+ 1.340(S-35) + 1.630\cdot 10^{-2}D + 1.675\cdot 10^{-7}D^2 \\ &- 1.025\cdot 10^{-2}T(S-35) - 7.139x10^{-13}TD^3, \end{aligned} \tag{6.10}$$

where T is temperature in °C, S is salinity in parts per thousand and D is depth in meters. It will give values in the range from 1435.2 to 1535.7 m/s with the parameter values for the various oceans of Fig. 3.7.

The formula will even predict the surprisingly high value of 1855 m/s for the Dead Sea (S=330 ppt, T=23 °C, D=0). This is not far from typical measured value of 1840 m/s, although the formula may not have been intended to be accurate for such a high salinity.

Fig. 6.2 shows that near the surface in warm waters, the speed of sound increases according to the second term of (6.10), $4.591T$. There is also an increase with temperature, e.g. $1.630 \cdot 10^{-2}D$, which means that there is a minimum at about 700 m depth. In Norwegian fjords in winter, on the other hand, with a cold surface and with fresh water from rivers on top, the higher speed of sound near the surface is not so prominent if it exists at all.

Accurate knowledge of the speed of sound is important in some imaging applications, like for exact focusing in synthetic aperture sonar [Hansen et al., 2011] and medical ultrasound [Austeng and Holm, 2002]. The effect of sound speed profiles in seawater is also that there will exist regions which are invisible to sonar. The existence and location of these regions vary with environmental parameters. This is the background for a cat-and-mouse game between sonars and military submarines that try to avoid being detected.

Sound waves will move towards the depth of the minimum sound speed. This channel of minimum velocity may stretch over long distances and form a waveguide for favorable sound propagation over thousands of km called the SOFAR (Sound Fixing and Ranging) channel, [Kuperman and Lynch, 2004].

6.2.2 Air

According to the ideal gas law, pressure varies with absolute temperature, T', and absolute volume, V', as $p' = nRT'/V$ where $R = 8314.51$ J/(mol K) is the universal gas constant and n is the number of moles. The density is also $\rho' = nM/V'$ where M is the molar mass of the gas, which for dry air is 0.0289645 kg/mol. Around the equilibrium point where $p' = p_0$ and $\rho' = \rho_0$, combination with (2.10) gives:

$$c_0 = \sqrt{\frac{K}{\rho_0}} = \sqrt{\gamma \frac{p_0}{\rho_0}} = \sqrt{\frac{\gamma k T'}{m}}, \tag{6.11}$$

where $k = 1.38064852 \cdot 10^{-23}$ J/K is Boltzmann's constant and the ratio of specific heats is $\gamma = c_p/c_v$ where c_p and c_v are the specific heat capacities under constant pressure and constant volume conditions respectively. The ratio is also called the adiabatic index and for an ideal diatomic gas it is $\gamma = 1.4$.

Example 6.3 Speed of sound in air. Letting temperature, T, be in °C rather than K by $T' = 273.15 + T$ results in

$$c_0 = \sqrt{\frac{273.15 \cdot \gamma k}{m}(1 + \frac{T}{273.15})} \approx 331.3 + 0.606 \cdot T. \tag{6.12}$$

This gives a value of 343.2 m/s at 20°C and 340.4 m/s at 15°C.

Normal pressure is $p_0 = 1.01 \cdot 10^5$ Pa and according to (2.10) this gives a bulk modulus of $K = 1.414 \cdot 10^5$ Pa. At 15°, the density can be found from (2.8) and the speed of sound and is $\rho_0 = K/c_0^2 = 1.22$ kg/m^3.

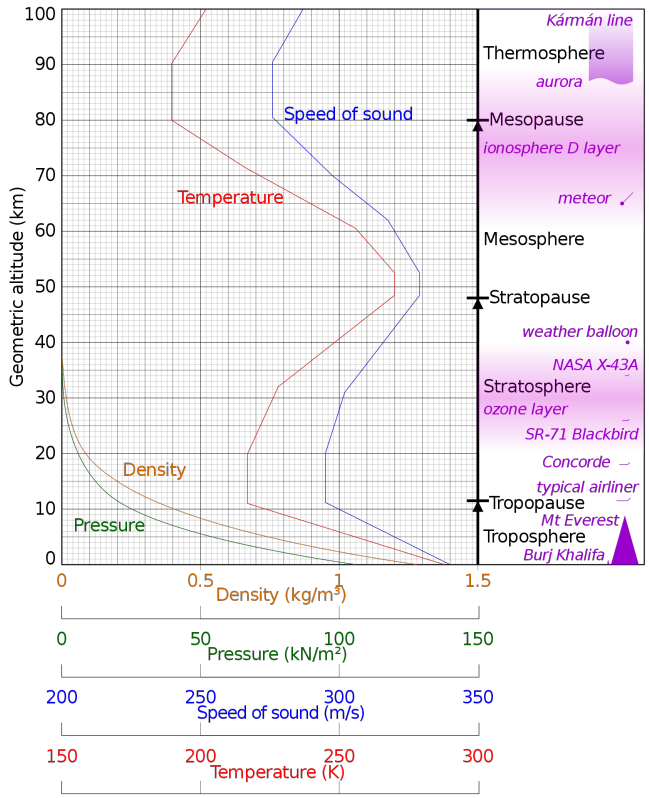

Figure 6.3 Density and pressure decrease smoothly with altitude, but temperature (red) does not. The speed of sound (blue) depends only on the complicated temperature variation at altitude and can be calculated from it since isolated density and pressure effects on the speed of sound cancel each other. Wikipedia: https://upload.wikimedia.org/wikipedia/commons/thumb/9/9d/Comparison_US_standard_atmosphere_1962.svg/1659px-Comparison_US_standard_atmosphere_1962.svg.png

Fig. 6.3 also shows density and pressure variations and their influence. Concentrating on the lowest 10 km, it is evident how temperature drops and so does speed of sound according to (6.12). Usually sound waves will therefore be bent up and into the atmosphere. Under special atmospheric conditions, called inversion, temperature may increase with height in the first km or so and speed of sound will increase with height, and waves will be bent back towards the surface and sound may carry longer. Elephants may for this reason communicate at infrasound frequencies over distances larger than 10 km at dusk or dawn [Larom et al., 1997].

Above the lowest 10 km, minima in the sound speed can be seen at heights 10–20 km and 80–90 km. Typically, there are either tropospheric (maximum at $\tilde{1}5$ km), stratospheric (maximum at $\tilde{5}0$ km), or thermospheric (maximum at $\tilde{1}00$ km) waveguides. These ducts are important for long range propagation of infrasound where absorption in air is small, see Fig. 3.8. The maxima in the speed of sound above these ducts will bend sound back to earth. This is important for e.g. verification of the nuclear test-ban treaty and for long term prediction of pressure events that are pre-cursors to changes in weather [Smets et al., 2015].

Chapter 7

From diffraction to the Fourier transform

This chapter starts with the Rayleigh-Sommerfeld integral and shows how the Fresnel and Fraunhofer zones for the near and far fields respectively can be seen as approximations to the integral. The Fourier transform relationship between an aperture function and the far field, which is a central concept in array signal processing, is also shown. This chapter builds on [Johnson and Dudgeon, 1992, Sect. 2.4].

7.1 Huygen's principle

Huygen's principle says that each point on a traveling wavefront can be considered as a secondary source of spherical radiation. Each such source will therefore spread according to the spatial part of the equation for spherical spreading in (2.16):

$$s(r,t) = \frac{A}{r}\exp\{\mathrm{i}(\omega t - kr)\}. \tag{7.1}$$

Adding up contributions, $s(\vec{x}_h)$, over an aperture, A, then results in:

$$s(\vec{x}) \propto \int\int_A s(\vec{x}_h)\frac{\exp\{\mathrm{i}kr\}}{r}\mathrm{d}A. \tag{7.2}$$

This principle is due to Christian Huygens, (1629-1695, Netherlands). The principle also expresses how an acoustic source like an oscillating piston is formed.

Other contributors to this field, which originally was concerned with optics, were:

- Joseph von Fraunhofer (D) 1787 - 1826
- Augustin Jean Fresnel (F) 1788 - 1827
- Gustav Robert Kirchhoff (D) 1824 –1887
- Lord Rayleigh, John William Strutt (GB) 1842 - 1919, Nobel prize physics, 1904.
- Arnold Johannes Wilhelm Sommerfeld (D) 1868 - 1951

7.2 Rayleigh–Sommerfeld diffraction formula

Eq. (7.2) captures the most essential part of diffraction, but the accurate formulation for the field from an aperture A is expressed in the Rayleigh-Sommerfeld diffraction formula, see [Goodman, 1996, Chap. 3]:

$$s(\vec{x}) = \frac{1}{\mathrm{i}\lambda}\int\int_A s(\vec{x}_h)\frac{\exp\{\mathrm{i}kr\}}{r}\cos\theta\mathrm{d}A. \tag{7.3}$$

It says that the wave at position $\vec{x}$ is a superposition of fields from the hole, due to the linearity of the wave equation as expressed in Huygen's principle. Each contribution is weighted by a spherical spreading function $\exp \mathrm{i}kr/r$. There is also weighting by $1/\lambda$. In addition there is an obliquity factor $\cos\theta$ and finally a phase shift of $\pi/2$ due to the factor $1/\mathrm{i}$.

There are two important approximations to the Rayleigh-Sommerfeld formula, the Fresnel approximation which is for the near field and small angles, and the Fraunhofer approximation which is valid in the far field. Inside the region where the Fresnel approximation is valid, the beam is **collimated**, i.e. it has the same diameter as the source itself. Some examples are x-ray beams in medical imaging and a laser point which maintains an almost constant beam width over the range of interest.

The following derivation leads to important estimates for the near field – far field transition distance. It also leads to the important result that there is a Fourier relationship between the aperture excitation and the field in the far field.

7.2.1 The Fresnel approximation

Eq. (7.3) is approximated for small angles by letting $\cos\theta \approx 1$ and $r \approx d$. This is substituted for the amplitude factor. But it cannot be used in the phase of the complex exponential as the end result is much more sensitive to approximations in the phase factor than in the amplitude factor.

For the phase the spherical surfaces are instead approximated by a quadratic function, therefore this is called a **parabolic** approximation:

$$\begin{aligned} r &= [(x-\tilde{x})^2 + (y-\tilde{y})^2 + d^2]^{1/2} = d[1 + \frac{(x-\tilde{x})^2 + (y-\tilde{y})^2}{d^2}]^{1/2} \\ &\approx d + \frac{(x-\tilde{x})^2 + (y-\tilde{y})^2}{2d}. \end{aligned} \tag{7.4}$$

This leads to:

$$s(x,y) \approx \frac{\exp\{\mathrm{i}kd\}}{\mathrm{i}\lambda d} \cdot \int\int_A s(\tilde{x},\tilde{y}) \exp\{\frac{\mathrm{i}k[(x-\tilde{x})^2 + (y-\tilde{y})^2]}{2d}\} d\tilde{x}d\tilde{y}. \tag{7.5}$$

The result is a **near field** approximation which is fine within approximately $\pm 15°$ of the axis perpendicular to the aperture, the z-axis. It is also called the **paraxial** approximation. It can only be used when the distance to position $\vec{x}$ doesn't vary too much over the aperture.

The Fresnel approximation expresses a 2D **convolution** between the field in the field in the original aperture and and transfer function $h(x,y)$:

$$h(x,y) = \frac{exp\{\mathrm{i}kd\}}{\mathrm{i}\lambda d} \exp\{\frac{\mathrm{i}k(x^2+y^2)}{2d}\} \tag{7.6}$$

This is a quadratic phase function which is the phase shift that a secondary wave encounters during propagation. More details about the Fresnel approximation can be found in [Goodman, 1996, Chap. 4.2].

7.2.2 Fraunhofer approximation

Here the phase term of the Fresnel approximation in Eq. (7.5) is expanded and the quadratic phase term variation over the aperture is neglected:

$$(x-\tilde{x})^2+(y-\tilde{y})^2 = x^2+y^2-2x\tilde{x}-2y\tilde{y}+\tilde{x}^2+\tilde{y}^2 \approx x^2+y^2-2x\tilde{x}-2y\tilde{y}. \tag{7.7}$$

If D is the maximum linear dimension of the aperture and d is the distance from source, then this is equivalent to assuming:

$$\frac{\tilde{x}^2}{2d} \leq \frac{(D/2)^2}{2d} << \lambda/2 => d >> \frac{D^2}{4\lambda}. \tag{7.8}$$

This is the definition of the Fresnel limit.

The Fraunhofer approximation is the result of inserting Eq. (7.7) in Eq. (7.5):

$$s(x,y) \approx \frac{\exp\{\mathrm{i}kd\}}{\mathrm{i}\lambda d}\exp\{\frac{\mathrm{i}k(x^2+y^2)}{2d}\}\cdot\int\int_A s(\tilde{x},\tilde{y})\exp\{\frac{\mathrm{i}k(x\tilde{x}+y\tilde{y})}{d}\}d\tilde{x}d\tilde{y}. \tag{7.9}$$

The result is a **far field** approximation which is valid far away from aperture. It should now be evident that $s(x,y)$ is the 2D **Fourier transform** of field in hole, $s(\tilde{x},\tilde{y})$.

In order to link it more directly to a Fourier transform between the aperture function and the wavenumber domain, imagine substituting new variables $k_{\tilde{x}} = k\tilde{x}/d$ and $k_{\tilde{y}} = k\tilde{y}/d$, changing the integral to $s(k_{\tilde{x}}, k_{\tilde{y}})$. In the end we therefore have an integral between the spatial aperture domain and the wavenumber domain [Johnson and Dudgeon, 1992, Chap. 2.4].

This result links the physics and the signal processing via the important Fourier transform. It is also the basis for a simplified expression like angular resolution $\theta \approx \lambda/D$, which says that a small aperture leads to wide beam and vice versa just like a short time-function has a wide spectrum in temporal signal processing.

More details about the Fraunhofer approximation can be found in [Goodman, 1996, Chap. 4.3].

7.3 Practical consequences of diffraction in ultrasound

7.3.1 Near field–far field limit

The transition from the near field to the far field is gradual in practice and there is no clear point where it takes place. Therefore there exists several limits which are used. Here they are listed according to increasing distance from the aperture or source:

- $d_F = D^2/(4\lambda)$: Fresnel limit of (7.8)
- $d = \pi r^2/\lambda = \pi/4 \cdot D^2/\lambda$: Diffraction limit
- $d_R = 2D^2/\lambda$: Rayleigh distance, maximum path length difference $\lambda/16$

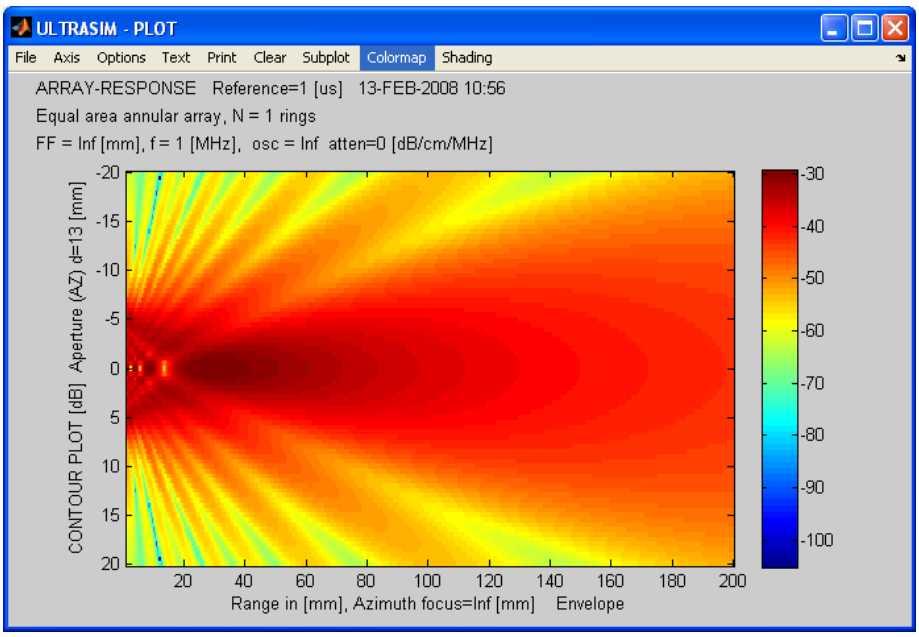

Figure 7.1 Acoustic field from a 1 MHz D =13 mm aperture unfocused transducer. Observe how the field starts transitioning to one with a uniform angle at depth $D^2/(4\lambda) \approx 28$ mm and that the transition is more or less complete at $\pi D^2/(4\lambda) \approx 88$ mm. Simulated with Ultrasim [Holm, 2001]

In all cases, the transition point distance is proportional to D^2/λ. The difference between the various criteria is the multiplication factor, which can be 0.25, 0.79, or 2. This is illustrated in Fig. 7.1 which is a simulation of a 1 MHz ultrasound with aperture 13 mm.

A simple interpretation and rule-of-thumb is that whenever the aperture tries to resolve objects that are smaller than the size of the aperture itself, the imaging takes place in the near field. This principle can be formulated by starting with the resolution of an aperture at a distance d_e which is θd_e, where the angular resolution is $\theta \approx \lambda/D$. Setting this equal to the size of the aperture gives:

☞ If the object is smaller than the aperture, the system is operating in the near field

$$D = \theta d = d_e \lambda / D \Rightarrow d_e = D^2/\lambda \tag{7.10}$$

7.3.2 Hard and soft baffle in acoustics

The validity of the Rayleigh Sommerfeld diffraction formula of Eq. (7.3) was tested against measurements for common ultrasound transducer elements in [Selfridge et al., 1980]. It was found that the $\cos\theta$ term indeed was important. The result was that the common formula for the far field pressure radiation pattern of a strip element of length d must be multiplied by the same factor:

$$p = p_0 \frac{\sin(\pi d/\lambda \sin\theta)}{\pi d/\lambda \sin\theta} X(\theta) \tag{7.11}$$

where the obliquity factor is $X(\theta) = \cos\theta$.

This is actually the soft baffle case in acoustics, where the surroundings of the acoustic element is such that the pressure is zero. The other case is a hard baffle, where the boundary condition outside the source has zero

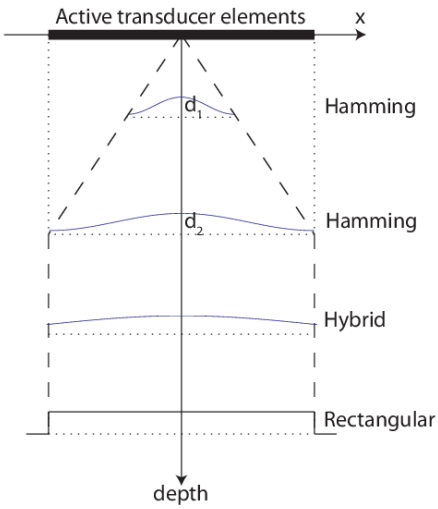

Figure 7.2 Dynamic aperture and dynamic weighting as typically used in medical ultrasound

particle velocity, and then the obliquity factor is just $X(\theta) = 1$. In [Szabo, 2014] (chapter 7) it is argued that in some cases even an average of the two, $X(\theta) = (1+\cos\theta)/2$ describes realistic transducer elements.

The three cases are also found in [Goodman, 1996, Chap. 3.6] where they correspond to three different approximations in the Kirchoff and Rayleigh-Sommerfeld formulations of diffraction:

$$X(\theta) = \begin{cases} \cos\theta, & \text{First Rayleigh-Sommerfeld solution} \\ 1, & \text{Second Rayleigh-Sommerfeld solution} \\ (1+\cos\theta)/2, & \text{Kirchoff theory.} \end{cases} \tag{7.12}$$

7.3.3 Lower limit for range

In ultrasound imaging, the small angle limit of the Fresnel approximation and the resulting approximation $r \approx d$, is expressed by the ratio of the distance and the aperture, $f_\# = d/D$. This is called the f-number.

The angle, θ, will be given by $\tan\theta/2 = (D/2)/d = 0.5/f_\#$. A rule-of-thumb is that the f-number should not be lower than 1 to 2, otherwise the image quality may actually deteriorate with a larger aperture. This corresponds to angles $\theta/2 = 14\ldots26.6°$ degrees which corresponds quite well with the previously stated limitation of the Fresnel theory at $\theta/2 \approx 15°$.

☞ The f-number should never be less than 1–2.

This limit is also justified by the mainlobe width of the resulting beam. It can for instance be found from Eq. (7.11) by finding the peak to zero distance which is $\sin\theta = \lambda/d$. Therefore the resolution at a distance D is $D\sin\theta \approx \lambda f_\#$. As $f_\#$ approaches 1, the resolution approaches the wavelength, λ, and the geometric wave propagation theory underlying eq. (7.11) breaks down.

This is the idea behind the concept of the expanding aperture often used in ultrasound imaging as shown in Fig. 7.2. It usually expands linearly with range or depth, maintaining a constant $f_\#$, out to the range where the full aperture is activated and from then on the full aperture is used.

Simultaneously the aperture weighting function is changed dynamically from a smooth function like a Hamming window to a rectangular one. The smooth function decreases sidelobes and increases image quality for objects near the transducer while the rectangular function maximizes sensitivity as the penetration limit is reached.

Chapter 8

Angular spectrum simulation of acoustic fields

The following sections will give an introduction to concepts which are important in practical numerical simulation methods.

8.1 Helmholtz equation

Equation (2.12) may be decomposed into a product of a spatial and a temporal term:

$$u(x,t) = U(x) \cdot T(t). \tag{8.1}$$

When inserted into the lossless wave equation of (2.11), one gets

$$\frac{\nabla^2 U}{U} = \frac{1}{c_0^2 T} \frac{\mathrm{d}^2 T}{\mathrm{d}t^2}. \tag{8.2}$$

Here the left-hand side only depends on the spatial variable, x, and the right-hand side only depends on time, t. Both sides must therefore be a constant, which we call $-k^2$ where k will be the wave number. The spatial equation then becomes:

$$\left(\nabla^2 + k^2\right) U \;=\; 0. \tag{8.3}$$

This is the Helmholtz equation.

8.2 Spatial impulse response or Green's function

Assume a 1-D lossless wave equation with a source term:

$$\nabla^2 u - \frac{1}{c_0^2} \frac{\partial^2 u}{\partial t^2} = S(x,t). \tag{8.4}$$

The Green's function is the spatial impulse response and therefore the solution is the convolution of the Green's function and the source term:

$$u(x,t) = \int_0^t \int_{-\infty}^{\infty} G(x-x', t-t') \cdot S(x', t')\, \mathrm{d}x'\, \mathrm{d}t' = G(x,t) * S(x,t) \tag{8.5}$$

The Green's function can be found analytically[1] and depends on the number of dimensions [Cox and Treeby, 2017]:

$$G_{1D}(x,t) = \frac{c_0}{2} \mathrm{u}(t - |x|/c_0), \tag{8.6}$$

$$G_{2D}(\vec{x},t) = \frac{\mathrm{u}(t - |\vec{x}|/c_0)}{2\pi\sqrt{t^2 - |\vec{x}|^2/c_0^2}}, \tag{8.7}$$

[1] see e.g. Wikipedia: https://en.wikipedia.org/wiki/Green%27s_function

$$G_{3D}(\vec{x}, t) = \frac{\delta(t - |\vec{x}|/c_0)}{4\pi|\vec{x}|}, \tag{8.8}$$

where $\mathrm{u}(t)$ and $\delta(t)$ are the unit step and impulse functions respectively.[2]

The Helmholtz equation of (8.3) has this Green's function in 3D:

$$G_{3D}(\vec{x}, t) = \frac{-\mathrm{e}^{-\mathrm{i}kr}}{4\pi r}, \quad r = |\vec{x}|, \tag{8.9}$$

which bears some resemblance to the spatial component of the solution to the spherical wave equation of (2.16).

The Green's function method is based on a linear, lossless theory, but losses may be added to the method as done in the Field II simulation program [Jensen et al., 1993].

8.3 The angular spectrum method

In the angular spectrum method for simulation, a plane wave is propagated in the z-direction. The method assumes that the field $U(x, y, z = z_0)$ in the $(x, y, z = z_0)$-plane is known and gives a method for finding $U(x, y, z)$ in a new parallel plane (x, y, z). This is done via the spatial Fourier transform in the (x, y)-plane.

The initial Fourier transform is:

$$A(u, v; z_0) = \iint_{-\infty}^{\infty} U(x, y, z_0) \exp[-\mathrm{i}2\pi(ux + uy)]\,\mathrm{d}x\,\mathrm{d}y. \tag{8.10}$$

The inverse transform shows how this is a decomposition of the field in a sum of plane waves:

$$U(x, y, z_0) = \iint_{-\infty}^{\infty} A(u, v; z_0) \exp[\mathrm{i}2\pi(ux + vy)]\,\mathrm{d}u\,\mathrm{d}v, \tag{8.11}$$

where $U(\cdot)$ is the spatial component of the field from (8.1).

The spatial frequencies[3] u and v relate to the components of the wave vector, $\vec{k}$, in a similar way as temporal frequency, f, relates to angular frequency $\omega = 2\pi f$. Thus $(u, v) = (k_x, k_y)/(2\pi)$. If a plane wave is propagating in directions (ϕ, θ) in spherical coordinates,[4] the components of the wave vector of (2.12) are [Latychevskaia and Fink, 2015]:

$$\vec{k} = \frac{2\pi}{\lambda}\left(\cos\phi\sin\theta, \sin\phi\sin\theta, \cos\theta\right) = 2\pi(u, v, w), \tag{8.12}$$

where θ is the polar angle, or angle with respect to the z-axis, ϕ is the azimuth angle, and w is the spatial frequency in the z-direction (not used here).

[2] Note difference between $u(t)$ - displacement, and $\mathrm{u}(t)$ - the unit step function

[3] Note that u and v without any argument are spatial frequencies

[4] For spherical to Cartesian transformation, see Wikipedia https://en.wikipedia.org/wiki/Spherical_coordinate_system#Cartesian_coordinates

The components of the wave vector are also called **direction cosines**,

$$\begin{aligned} \alpha &= \cos\phi \sin\theta, \\ \beta &= \sin\phi \sin\theta, \\ \gamma &= \cos\theta, \end{aligned} \tag{8.13}$$

and where $\alpha^2 + \beta^2 + \gamma^2 = 1$. Therefore the Fourier transform, $A(u, v; 0)$, is a decomposition of the field, $U(x, y, 0)$, in plane wave components at different angles. It is therefore called the angular spectrum.

8.3.1 The diffraction step

We want to propagate the field via the angular spectrum in order to find

$$U(x, y, z) = \iint_{-\infty}^{\infty} A(u, v; z) \exp[\mathrm{i}2\pi(ux + vy)] \, \mathrm{d}u \, \mathrm{d}v. \tag{8.14}$$

The condition is that the field has to satisfy the Helmholtz equation of (8.3) which takes care of diffraction. It is shown in [Goodman, 1996, Chap. 3.10] that the new angular spectrum then can be found as

$$A(u, v; z) = A(u, v; z_0) \cdot \exp\left(\mathrm{i}\frac{2\pi}{\lambda} z \sqrt{1 - \alpha^2 - \beta^2}\right). \tag{8.15}$$

As long as the expression in the square root of (8.15) is positive so $\gamma = \cos\theta \leq 1$ there will be a real propagation angle, θ, relative to the z-axis. Propagation will then only change the phase of the component of the angular spectrum and not the amplitude.

However, if $\alpha^2 + \beta^2 > 1$, the propagation factor becomes a real exponential and the angular spectrum component will be attenuated. These non-propagating wave components are called **evanescent waves**.

The Angular Spectrum Approach (ASA) algorithm is illustrated in Fig. 8.1.

8.3.2 Attenuation and nonlinearity

The angular spectrum method as presented builds on Helmholtz equation. Therefore the operator of (8.15) only accounts for diffraction between each step in the simulation and is only valid for a single frequency. Broad-band signals may be handled by propagating several frequencies, and attenuation, dispersion, refraction, and nonlinearity may also be included in the substep assuming that their effects are small.

When nonlinearity is included, many harmonics of the initial fundamental frequency will have to be propagated per substep. A method that accounts for the physics of diffraction, attenuation and nonlinearity is given in [Christopher and Parker, 1991], even for axis symmetric sources. In that case the 2-D Fourier transform of (8.14) is substituted with a 1-D discrete Hankel transform for computational efficiency. The 1-D Hankel transform method was used for the nonlinear simulations of [Synnevåg and Holm, 1998] and [Prieur et al., 2012].

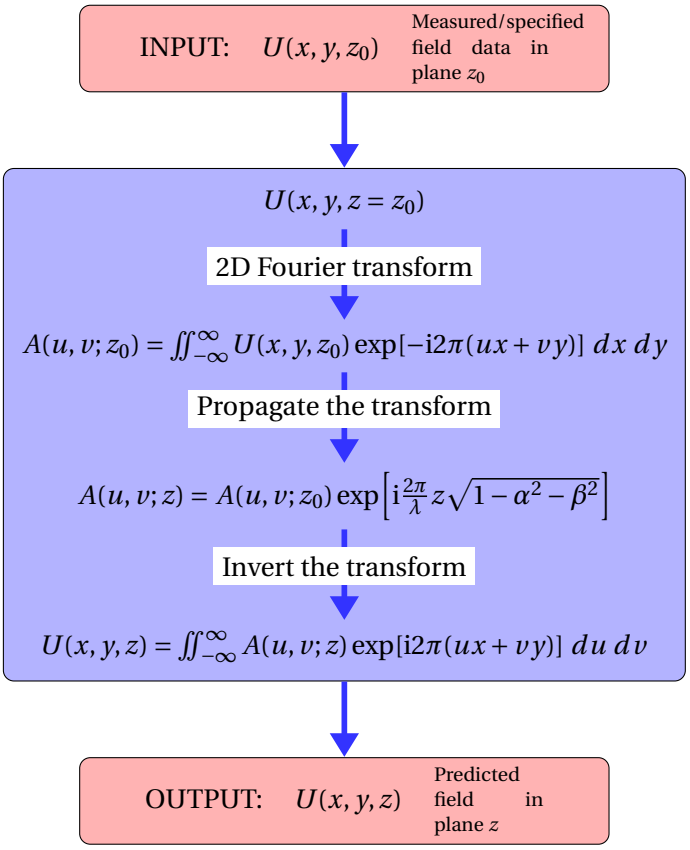

Figure 8.1 Illustration of the Angular Spectrum Approach algorithm (from Andreas Austeng)

The k-Wave simulation program is based on a pseudo-spectral method which can account for attenuation, dispersion, and refraction. It uses fractional derivatives indirectly because the attenuation model is expressed with a modification of the fractional Laplacian of [Chen and Holm, 2004] which was developed in [Treeby et al., 2012]. The fractional Laplacian is a fractional derivative in space rather than time.

Appendix A

Approximations and terminology

A.1 Power series approximation

One version of Newton's generalized binomial theorem is [Rottmann, 2003]:

$$(1+x)^{n/m} = 1 + \frac{n}{m}x - \frac{n(m-n)}{2!m^2}x^2 + \frac{n(m-n)(2m-n)}{3!m^3}x^3 + \cdots \tag{A.1}$$

Often used approximations are based on keeping only the first two or three terms and are valid when $x \ll 1$:

$$\frac{1}{1+x} = (1+x)^{-1} \approx 1 - x + x^2 + \cdots \tag{A.2}$$

$$\sqrt{1+x} = (1+x)^{1/2} \approx 1 + \frac{x}{2} - \frac{x^2}{8} + \frac{x^3}{16} - \cdots \tag{A.3}$$

$$1/\sqrt{1+x} = (1+x)^{-1/2} \approx 1 - \frac{x}{2} + \frac{3}{8}x^2 - \frac{5}{16}x^3 + \cdots \tag{A.4}$$

A.2 McLaurin series for trigonometric functions

The argument is always expressed in radians in these formulas:

$$\sin\theta = \theta - \frac{1}{3!}\theta^3 + \frac{1}{5!}\theta^5 - \cdots \tag{A.5}$$

$$\cos\theta = 1 - \frac{1}{2!}\theta^2 + \frac{1}{4!}\theta^4 - \cdots \tag{A.6}$$

$$\tan\theta = \theta + \frac{1}{3}\theta^3 + \frac{2}{15}\theta^5 - \cdots \tag{A.7}$$

The small angle approximations use only a single term:

$$\sin\theta \approx \tan\theta \approx \theta \tag{A.8}$$

$$\cos\theta \approx 1 \tag{A.9}$$

When the argument $\theta < 0.2$ radians $\approx 11.50°$ the error in $\sin\theta$ is less than 0.7 %, the error in $\tan\theta$ is less than 1.4 %, and the error in $\cos\theta$ is less than 2 %. In practice the approximate formulas are useful up to approximately 0.25 radians or 15°.

A.3 Norwegian terminology

- Bølgeligningen
- Planbølger, sfæriske bølger
- Propagerende bølger, bølgetall
- Sinking/sakking: $\vec{\alpha}$
- Dispersjon
- Attenuasjon eller demping
- Refraksjon
- Ikke-linearitet
- Diffraksjon; nærfelt, fjernfelt
- Gruppeantenne (= array)

Kilde: Bl.a. [Hovem, 1999].

Bibliography

[Abel, 1823] Abel, N. H. (1823). Oplösning af et par opgaver ved hjelp af bestemte integraler (Solution of a couple of problems by means of definite integrals). *Magazin for naturvidenskaberne*, 2(55):2.

[Ainslie and McColm, 1998] Ainslie, M. and McColm, J. G. (1998). A simplified formula for viscous and chemical absorption in sea water. *J. Acoust. Soc. Am.*, 103(3):1671–1672.

[Allen et al., 1948] Allen, C., Frings, H., and Rudnick, I. (1948). Some biological effects of intense high frequency airborne sound. *J. Acoust. Soc. Am.*, 20(1):62–65.

[Austeng and Holm, 2002] Austeng, A. and Holm, S. (2002). Sparse 2-d arrays for 3-d phased array imaging-experimental validation. *IEEE Trans. Ultrason. Ferroelectr., Freq. Control*, 49(8):1087–1093.

[Bamber, 2004] Bamber, J. C. (2004). Attenuation and absorption. In *Physical Principles of Medical Ultrasonics (eds C. R. Hill, J. C. Bamber and G. R. ter Haar), 2nd Ed.*, chapter 4, pages 93–166. John Wiley & Sons, Chichester, UK.

[Bass et al., 1972] Bass, H. E., Bauer, H.-J., and Evans, L. B. (1972). Atmospheric absorption of sound: Analytical expressions. *J. Acoust. Soc. Am.*, 52(3B):821–825.

[Blackstock, 2000] Blackstock, D. T. (2000). *Fundamentals of physical acoustics*. John Wiley & Sons, New York.

[Blair and Reiner, 1951] Blair, G. S. and Reiner, M. (1951). The rheological law underlying the Nutting equation. *Appl. Sci. Res.*, 2(1):225–234.

[Broedersz and MacKintosh, 2014] Broedersz, C. P. and MacKintosh, F. C. (2014). Modeling semiflexible polymer networks. *Rev Mod Phys*, 86(3):995.

[Buckingham, 2000] Buckingham, M. J. (2000). Wave propagation, stress relaxation, and grain-to-grain shearing in saturated, unconsolidated marine sediments. *J. Acoust. Soc. Am.*, 108(6):2796–2815.

[Buckingham, 2007] Buckingham, M. J. (2007). On pore-fluid viscosity and the wave properties of saturated granular materials including marine sediments. *J. Acoust. Soc. Am.*, 122(3):1486–1501.

[Caputo, 1967] Caputo, M. (1967). Linear models of dissipation whose Q is almost frequency independent–II. *Geophys. J. Int.*, 13(5):529–539.

[Carstensen et al., 1953] Carstensen, E. L., Li, K., and Schwan, H. P. (1953). Determination of the acoustic properties of blood and its components. *J. Acoust. Soc. Am.*, 25(2):286–289.

[Chandrasekaran et al., 2023] Chandrasekaran, S. N., Holm, S., and Näsholm, S. P. (2023). Wave equations of the two common sediment acoustic theories. In *Proc. Meet. Acoust.*, volume 51. AIP Publishing.

[Chen and Holm, 2004] Chen, W. and Holm, S. (2004). Fractional Laplacian time-space models for linear and nonlinear lossy media exhibiting arbitrary frequency power-law dependency. *J. Acoust. Soc. Am.*, 115(4):1424–1430.

[Christopher and Parker, 1991] Christopher, P. T. and Parker, K. J. (1991). New approaches to nonlinear diffractive field propagation. *J. Acoust. Soc. Am.*, 90(1):488–499.

[Cox and Treeby, 2017] Cox, B. and Treeby, B. (2017). Ultrasound in medicine.

[Dahl et al., 2007] Dahl, P. H., Miller, J. H., Cato, D. H., and Andrew, R. K. (2007). Underwater ambient noise. *Acoustics Today*, 3(1):23–33.

[Duck, 2012] Duck, F. A. (2012). *Physical properties of tissues: a comprehensive reference book*. Academic press.

[Evans et al., 1972] Evans, L. B., Bass, H. E., and Sutherland, L. C. (1972). Atmospheric absorption of sound: theoretical predictions. *J. Acoust. Soc. Am.*, 51(5B):1565–1575.

[Feynman, 1967] Feynman, R. P. (1967). *The character of physical law*. MIT press.

[Gemant, 1936] Gemant, A. (1936). A method of analyzing experimental results obtained from elasto-viscous bodies. *Physics*, 7(8):311–317.

[Goodman, 1996] Goodman, J. W. (1996). Introduction to Fourier optics, second edition. *New York*.

[Gross, 1996] Gross, D. J. (1996). The role of symmetry in fundamental physics. *Proc. Nat. Acad. Sci. USA*, 93(25):14256–14259.

[Hamilton and Blackstock, 1988] Hamilton, M. F. and Blackstock, D. T. (1988). On the coefficient of nonlinearity β in nonlinear acoustics. *J. Acoust. Soc. Am.*, 83(1):74–77.

[Hamilton and Blackstock, 2008] Hamilton, M. F. and Blackstock, D. T. (2008). *Nonlinear Acoustics*. Acoust. Soc. Am. Press, New York.

[Hansen et al., 2011] Hansen, R. E., Callow, H. J., Sabo, T. O., and Synnes, S. A. V. (2011). Challenges in seafloor imaging and mapping with synthetic aperture sonar. *IEEE Trans Geosci Rem Sens*, 49(10):3677–3687.

[Holland and Dosso, 2022] Holland, C. W. and Dosso, S. E. (2022). Hamilton's geoacoustic model. *J. Acoust. Soc. Am.*, 151(1):R1–R2.

[Holm, 2001] Holm, S. (2001). Ultrasim-a toolbox for ultrasound field simulation. In *Proc. Nordic Matlab Conference, Oslo, Norway*.

[Holm, 2012] Holm, S. (2012). Ultrasound positioning based on time-of-flight and signal strength. In *Int. Conf. Indoor Pos. Indoor Nav. (IPIN)*, pages 1–6. IEEE.

[Holm, 2019a] Holm, S. (2019a). Dispersion analysis for wave equations with fractional laplacian loss operators. *Fract Calc Appl Anal*, 22(6):1596–1606.

[Holm, 2019b] Holm, S. (2019b). *Waves with power-law attenuation*. Springer and ASA Press, Switzerland.

[Holm, 2020] Holm, S. (2020). Time domain characterization of the Cole-Cole dielectric model. *J. Electr. Bioimp.*, 11(1):101–105.

[Holm et al., 2023] Holm, S., Chandrasekaran, S. N., and Näsholm, S. P. (2023). Adding a low frequency limit to fractional wave propagation models. *Front. Phys.*, 11.

[Holm et al., 2005] Holm, S., Hovind, O. B., Rostad, S., and Holm, R. (2005). Indoors data communications using airborne ultrasound. In *IEEE Int. Conf. Acoust. Speech Sign. Proc.*, pages 957–960.

[Holm and Näsholm, 2011] Holm, S. and Näsholm, S. P. (2011). A causal and fractional all-frequency wave equation for lossy media. *J. Acoust. Soc. Am.*, 130(4):2195–2202.

[Hovem, 1999] Hovem, J. M. (1999). *Marin akustikk.* NTNU, Trondheim, Norway.

[Jensen et al., 1993] Jensen, J. A., Gandhi, D., and WD Jr, O. (1993). Ultrasound fields in an attenuating medium. In *Proc IEEE Ultrason Symp*, pages 943–946. IEEE.

[Johnson and Dudgeon, 1992] Johnson, D. H. and Dudgeon, D. E. (1992). *Array signal processing: Concepts and techniques.* Simon & Schuster.

[Kinsler et al., 1999] Kinsler, L. E., Frey, A. R., Coppens, A. B., and Sanders, J. V. (1999). *Fundamentals of acoustics.* Wiley-VCH, New York. 4th Edition.

[Kollmannsberger and Fabry, 2011] Kollmannsberger, P. and Fabry, B. (2011). Linear and nonlinear rheology of living cells. *Ann. Rev. Mater. Res.*, 41:75–97.

[Kuperman and Lynch, 2004] Kuperman, W. A. and Lynch, J. F. (2004). Shallow-water acoustics. *Physics Today*, 57(10):55–61.

[Kwan et al., 2002] Kwan, A., Dudley, J., and Lantz, E. (2002). Who really discovered Snell's law? *Physics World*, 15(4):64.

[Landau and Lifshitz, 1976] Landau, L. D. and Lifshitz, E. M. (1976). *Mechanics, 3rd Edition: Vol. 1 of Course of Theoretical Physics.* Elsevier.

[Landau and Lifshitz, 1987] Landau, L. D. and Lifshitz, E. M. (1987). *Fluid Mechanics, 3rd Edition: Vol. 6 of Course of Theoretical Physics.* Elsevier.

[Larom et al., 1997] Larom, D., Garstang, M., Payne, K., Raspet, R., and Lindeque, M. (1997). The influence of surface atmospheric conditions on the range and area reached by animal vocalizations. *J Exp Biol*, 200(3):421–431.

[Latychevskaia and Fink, 2015] Latychevskaia, T. and Fink, H.-W. (2015). Practical algorithms for simulation and reconstruction of digital in-line holograms. *Appl Opt*, 54(9):2424–2434.

[Liouville, 1832] Liouville, J. (1832). Mémoire sur quelques questions de géométrie et de mécanique, et sur un nouveau genre de calcul pour résoudre ces questions (Memo on some questions of geometry and mechanics and on a new kind of calculus to resolve these questions). *J. Ec. Polytech.*, 13:1–400.

[Mackenzie, 1981] Mackenzie, K. V. (1981). Nine-term equation for sound speed in the oceans. *J. Acoust. Soc. Am.*, 70(3):807–812.

[Näsholm, 2013] Näsholm, S. P. (2013). Model-based discrete relaxation process representation of band-limited power-law attenuation. *J. Acoust. Soc. Am.*, 133(3):1742–1750.

[Nutting, 1921] Nutting, P. (1921). A new general law of deformation. *J. Franklin. Inst.*, 191(5):679–685.

[Pandey and Holm, 2016] Pandey, V. and Holm, S. (2016). Connecting the grain-shearing mechanism of wave propagation in marine sediments to fractional order wave equations. *J. Acoust. Soc. Am.*, 140:4225–4236.

[Peatross and Ware, 2015] Peatross, J. and Ware, M. (2015). *Physics of Light and Optics.* available at optics.byu.edu.

[Podlubny et al., 2017] Podlubny, I., Magin, R. L., and Trymorush, I. (2017). Niels Henrik Abel and the birth of fractional calculus. *Fract. Calc. Appl. Anal.*, 20(5):1068–1075.

[Prieur et al., 2012] Prieur, F., Nasholm, S. P., Austeng, A., Tichy, F., and Holm, S. (2012). Feasibility of second harmonic imaging in active sonar: measurements and simulations. *IEEE J. Ocean. Eng.*, 37(3):467–477.

[Riewe, 1996] Riewe, F. (1996). Nonconservative Lagrangian and Hamiltonian mechanics. *Phys. Rev. E*, 53(2):1890.

[Rottmann, 2003] Rottmann, K. (2003). *Matematisk formelsamling (Mathematical formulas)*. Spektrum forlag.

[Santucci et al., 2006] Santucci, S., Fioretto, D., Comez, L., Gessini, A., and Masciovecchio, C. (2006). Is there any fast sound in water? *Phys. Rev. Lett.*, 97(22):225701.

[Selfridge et al., 1980] Selfridge, A., Kino, G., and Khuri-Yakub, B. (1980). A theory for the radiation pattern of a narrow-strip acoustic transducer. *Appl. Phys. Lett.*, 37(1):35–36.

[Shen et al., 2011] Shen, Z. L., Kahn, H., Ballarini, R., and Eppell, S. J. (2011). Viscoelastic properties of isolated collagen fibrils. *Biophys. J.*, 100(12):3008–3015.

[Siegmund-Schultze, 2016] Siegmund-Schultze, R. (2016). Pulling Harriot out of Newton's shadow: How the Norwegian outsider Johannes Lohne came to contribute to mainstream history of mathematics. In *Historiography of Mathematics in the 19th and 20th Centuries*, pages 219–243. Springer.

[Smets et al., 2015] Smets, P., Evers, L., Näsholm, S., and Gibbons, S. (2015). Probabilistic infrasound propagation using realistic atmospheric perturbations. *Geophys Res Lett*, 42(15):6510–6517.

[Stokes, 1845] Stokes, G. G. (1845). On the theories of the internal friction of fluids in motion, and of the equilibrium and motion of elastic solids. *Trans. Cambridge Philos. Soc.*, 8 (part III):287–319.

[Synnevåg and Holm, 1998] Synnevåg, J.-F. and Holm, S. (1998). Non-linear propagation of limited diffraction beams [in medical us imaging]. In *IEEE Ultrason Symp Proc*, pages 1885–1888.

[Szabo, 2014] Szabo, T. L. (2014). *Diagnostic Ultrasound Imaging: Inside Out, Second Ed.* Academic Press.

[Szabo and Wu, 2000] Szabo, T. L. and Wu, J. (2000). A model for longitudinal and shear wave propagation in viscoelastic media. *J. Acoust. Soc. Am.*, 107:2437–2446.

[Trachenko et al., 2020] Trachenko, K., Monserrat, B., Pickard, C., and Brazhkin, V. (2020). Speed of sound from fundamental physical constants. *Sci Adv*, 6(41):eabc8662.

[Treeby and Cox, 2010] Treeby, B. E. and Cox, B. T. (2010). Modeling power law absorption and dispersion for acoustic propagation using the fractional Laplacian. *J. Acoust. Soc. Am.*, 127:2741–2748.

[Treeby et al., 2012] Treeby, B. E., Jaros, J., Rendell, A. P., and Cox, B. T. (2012). Modeling nonlinear ultrasound propagation in heterogeneous media with power law absorption using a k-space pseudospectral method. *J. Acoust. Soc. Am.*, 131(6):4324–4336.

[Tschoegl, 1989] Tschoegl, N. W. (1989). *The phenomenological theory of linear viscoelastic behavior: An introduction.* Springer-Verlag, Berlin. Reprinted in 2012.

[Versluis et al., 2000] Versluis, M., Schmitz, B., Von der Heydt, A., and Lohse, D. (2000). How snapping shrimp snap: through cavitating bubbles. *Science*, 289(5487):2114–2117.